Published for SISSA by Springer

Received: *September 20, 2022*
Accepted: *January 13, 2023*
Published: *June 27, 2023*

Measurement of single top-quark production in the s-channel in proton–proton collisions at $\sqrt{s} = 13$ TeV with the ATLAS detector

The ATLAS collaboration

E-mail: atlas.publications@cern.ch

Abstract: A measurement of single top-quark production in the s-channel is performed in proton–proton collisions at a centre-of-mass energy of 13 TeV with the ATLAS detector at the CERN Large Hadron Collider. The dataset corresponds to an integrated luminosity of 139 fb^{-1}. The analysis is performed on events with an electron or muon, missing transverse momentum and exactly two b-tagged jets in the final state. A discriminant based on matrix element calculations is used to separate single-top-quark s-channel events from the main background contributions, which are top-quark pair production and W-boson production in association with jets. The observed (expected) signal significance over the background-only hypothesis is 3.3 (3.9) standard deviations, and the measured cross-section is $\sigma = 8.2^{+3.5}_{-2.9}$ pb, consistent with the Standard Model prediction of $\sigma^{\mathrm{SM}} = 10.32^{+0.40}_{-0.36}$ pb.

Keywords: Hadron-Hadron Scattering, Top Physics

ArXiv ePrint: 2209.08990

https://doi.org/10.1007/JHEP06(2023)191

JHEP06(2023)191

Contents

JHEP06(2023)191

1 Introduction

In proton–proton (pp) collisions, top quarks are produced predominantly in pairs via the strong interaction, but also singly via the electroweak interaction through a Wtb vertex. Single top-quark production is therefore a powerful probe for the top quark electroweak couplings. In the Standard Model (SM), three different production mechanisms are possible at leading-order (LO) in perturbative theory: an exchange of a virtual W boson either in the t-channel or in the s-channel, or the associated production of a top quark and a W boson (tW). Figure 1 shows the dominant Feynman diagram for s-channel single top-quark production, in which a top quark is produced with a bottom anti-quark in the final state. This mode plays an important role in searches for new phenomena that could be modelled as anomalous couplings or in effective field theories [1, 2].

Single top-quark production in proton–antiproton collisions was first observed by the CDF and D0 collaborations in combined measurements of the s-channel and t-channel [3, 4]. The s-channel production mode alone was later observed in a combination of the results from the two collaborations [5]. At the Large Hadron Collider (LHC), the production of single top quarks in pp collisions was observed by the CMS and ATLAS collaborations in t-channel production at a centre-of-mass energy of $\sqrt{s}$ = 7 TeV [6, 7], and in tW associated production at $\sqrt{s}$ = 8 TeV [8, 9]. Both production modes were later measured at

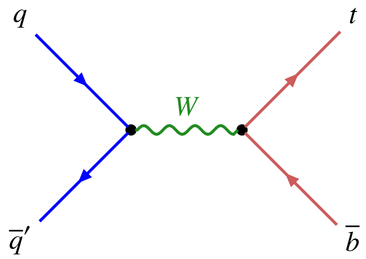

Figure 1. Feynman diagram for the dominant hard scattering process at leading-order in QCD of s-channel single top-quark production. The quarks in the initial (final) state are shown in blue (red), and the exchanged W boson is shown in green.

$\sqrt{s}$ = 13 TeV [10–13]. For s-channel production, searches were performed by the CMS Collaboration, combining $\sqrt{s} = 7$ TeV and $\sqrt{s} = 8$ TeV data, leading to an observed (expected) significance of 2.5 (1.1) standard deviations [14], and by the ATLAS Collaboration with $\sqrt{s} = 8$ TeV data, leading to an observed (expected) significance of 3.2 (3.9) standard deviations [15], over the background-only hypothesis.

In this paper, a measurement of the single-top-quark s-channel production cross-section in pp collisions at $\sqrt{s} = 13$ TeV is presented. In the SM, the s-channel single-top-quark cross-section in pp collisions at $\sqrt{s} = 13$ TeV, calculated at next-to-leading order (NLO) in quantum chromodynamics (QCD), is $\sigma^{\mathrm{SM}} = 10.32^{+0.40}_{-0.36}$ pb (cf. section 3). The increase in the cross-section for this process between $\sqrt{s} = 8$ TeV and $\sqrt{s} = 13$ TeV is slightly larger than for W-boson production, which is the second dominant source of background; it is however not as large as for $t\bar{t}$ production, which is the dominant source. Using predictions based on the same techniques as those described in section 3, the ratio of the s-channel single-top-quark cross-section to the W-boson cross-section is $1.4\,10^{-4}$ ($1.7\,10^{-4}$), and to the $t\bar{t}$ cross-section is $2.1\,10^{-2}$ ($1.2\,10^{-2}$), at $\sqrt{s} = 8$ TeV ($\sqrt{s} = 13$ TeV). This analysis is therefore more challenging as the centre-of-mass energy increases.

The top quark decays almost exclusively into a W boson and a b-quark. This analysis considers only the leptonic decays (electron or muon) of the W boson, because the fully hadronic final states are dominated by multijet background. Some of the events containing a W boson decaying into a τ-lepton which subsequently decays leptonically are also selected. At LO the final state contains two jets with large transverse momenta: one jet containing b-hadrons (called a b-jet) originating from the decay of the top quark into a b-quark, and another b-jet from the Wtb vertex producing the top quark. Thus the experimental signature consists of an isolated electron or muon, large missing transverse momentum due to the undetected neutrino from the W-boson decay, and two jets with large transverse momentum (p_{T}) which are both identified as containing b-hadrons (b-tagged). To extract the signal events amidst the copious background, a 'matrix element method' discriminant [16, 17] is used, which assigns to each selected event a probability of being signal, estimated by means of exact matrix element calculations at LO for signal and background processes. This strategy has been shown to provide better sensitivity than the boosted decision trees used in previous searches for s-channel production [15, 18].

2 ATLAS detector

ATLAS [19] is a multipurpose particle detector at the LHC with a forward–backward symmetric cylindrical geometry and a near 4π coverage in solid angle.[1] It consists of an inner tracking detector surrounded by a thin superconducting solenoid providing a 2 T axial magnetic field, electromagnetic and hadron calorimeters, and a muon spectrometer. The inner tracking detector covers the pseudorapidity range $|\eta| < 2.5$. It consists of silicon pixel, silicon microstrip, and transition radiation tracking detectors. Lead/liquid-argon (LAr) sampling calorimeters provide electromagnetic (EM) energy measurements with high granularity. A steel/scintillator-tile hadron calorimeter covers the central pseudorapidity range ($|\eta| < 1.7$). The endcap and forward regions are instrumented with LAr calorimeters for both the EM and hadronic energy measurements up to $|\eta| = 4.9$. The muon spectrometer surrounds the calorimeters and is based on three large superconducting air-core toroidal magnets with eight coils each. The field integral of the toroids ranges between 2.0 and 6.0 T m across most of the detector. The muon spectrometer includes a system of precision tracking chambers and fast detectors for triggering. A two-level trigger system is used to select events. The first-level trigger is implemented in hardware and uses a subset of the detector information to accept events at a rate below 100 kHz. This is followed by a software-based trigger that reduces the accepted event rate to 1 kHz on average depending on the data-taking conditions. An extensive software suite [20] is used in the reconstruction and analysis of real and simulated data, in detector operations, and in the trigger and data acquisition systems of the experiment.

3 Data and simulation samples

The data for this analysis were collected with the ATLAS detector at the LHC between 2015 and 2018, in pp collisions at $\sqrt{s} = 13$ TeV, using single-lepton triggers, and correspond to an integrated luminosity of 139 fb^{-1}. Only events for which the LHC beams were in stable-collision mode and all relevant subsystems were operational are considered [21].

Monte Carlo (MC) simulation is used to model signal and background processes. Events were simulated using either the full ATLAS detector simulation [22] based on Geant4 [23] or a faster simulation where the full Geant4 simulation of the calorimeter response is replaced by a detailed parameterisation of the shower shapes [22]. To simulate the effects of multiple interactions in the same and neighbouring bunch crossings (pile-up), additional interactions were generated using Pythia 8.186 [24] with a set of tuned parameters called the A3 tune [25] and overlaid onto the simulated hard-scatter event. Simulated events are reweighted to match the pile-up conditions observed in the full dataset, and are processed through the same reconstruction algorithms and analysis chain as the data.

[1] ATLAS uses a right-handed coordinate system with its origin at the nominal interaction point (IP) in the centre of the detector and the z-axis along the beam pipe. The x-axis points from the IP to the centre of the LHC ring, and the y-axis points upwards. Cylindrical coordinates (r, ϕ) are used in the transverse plane, ϕ being the azimuthal angle around the z-axis. The rapidity is defined as $y = (1/2)\ln[(E + p_z)/(E - p_z)]$ where E is the energy and p_z is the longitudinal component of the momentum along the beam pipe. The pseudorapidity is defined in terms of the polar angle θ as $\eta = -\ln\tan(\theta/2)$. Angular distance is measured in units of $\Delta R \equiv \sqrt{(\Delta\eta)^2 + (\Delta\phi)^2}$.

JHEP06(2023)191

Events of single-top-quark s-channel, t-channel, and tW events, as well as $t\bar{t}$ events, were generated at NLO in QCD using the POWHEG BOX v2 generator [26–32] for the nominal prediction of these processes. The top-quark mass was set to $m_t = 172.5\,\text{GeV}$. For single-top-quark s-channel and tW production, and for $t\bar{t}$ production, the samples were generated in the five-flavour scheme and using the NNPDF3.0NLO parton distribution function (PDF) sets [33], and for single-top-quark t-channel production, the samples were generated in the four-flavour scheme and using the NNPDF3.0NLO_nf4 PDF sets. The parton shower, hadronisation, and underlying event were added using PYTHIA 8.230 with the A14 tune [34] and the NNPDF2.3LO PDF sets [35]. The decays of b- and c-hadrons were simulated using the EVTGEN 1.6.0 program [36]. For $t\bar{t}$ production, the h_{damp} parameter[2] in POWHEG BOX was set to $1.5 \cdot m_t$. For tW production, the diagram removal (DR) scheme, in which all doubly resonant NLO tW diagram amplitudes are removed [37], was employed to handle interference with $t\bar{t}$ diagrams.

Alternative simulation samples are used to estimate modelling uncertainties of top-quark processes (cf. section 7). For the dominant $t\bar{t}$ background process, two alternative samples are used: one produced with POWHEG BOX v2 but with the h_{damp} parameter set to $3 \cdot m_t$ in order to estimate the impact of varying the resummation, and the other produced with MADGRAPH5_AMC@NLO to assess the effect of changing the matching of NLO matrix elements (MEs) to the parton shower. For tW production, another sample produced with POWHEG BOX v2 but using the diagram subtraction scheme, where a gauge-invariant subtraction term modifies the NLO tW cross-section to locally cancel out the $t\bar{t}$ contribution [37], is used to evaluate the impact of using a different algorithm to remove the overlap with $t\bar{t}$ production. For these three samples, PYTHIA 8.230 is used for the parton shower and hadronisation. Furthermore, for each of the four top-quark processes, another sample was produced with POWHEG BOX v2 with the same settings as for the nominal POWHEG BOX + PYTHIA 8 samples, but with HERWIG 7.04 instead of PYTHIA 8.230 in order to assess the impact of using a different parton shower and hadronisation model. These samples used the H7UE tune [38, 39] and MMHT2014LO PDF set [40] with HERWIG 7.04, and EVTGEN 1.6.0 for b- and c-hadrons decays.

Samples of leptonic W- and Z-boson (V) events where the boson decays leptonically, and semileptonic diboson (VV) events where one boson decays leptonically and the other hadronically, were simulated with the SHERPA 2.2.1 [41] generator. In the Z-boson events samples, the invariant mass of the two leptons are required to be larger than 40 GeV. For V production, MEs with NLO (LO) accuracy in QCD for up to two (four) parton emissions were used, while for VV production, MEs with NLO (LO) accuracy for up to one (three) parton emission(s) were used. The MEs were calculated with the Comix [42] and OPENLOOPS [43–45] libraries, and matched to the SHERPA parton shower [46] using the MEPS@NLO prescription [47–50]. The NNPDF3.0NNLO set of PDFs was used, along with a dedicated set of tuned parton-shower parameters developed by the SHERPA authors.

The simulated event samples above described are normalised to the integrated luminosity corresponding to the analysed data sample, and using theory predictions for the

[2]The h_{damp} parameter is a resummation damping factor and one of the parameters that control the matching of POWHEG matrix elements to the parton shower and thus effectively regulates the high-p_{T} radiation against which the $t\bar{t}$ system recoils.

JHEP06(2023)191

cross-sections of the individual processes, as described below. The predicted cross-section for the s-channel single-top-quark signal is $\sigma^{\mathrm{SM}} = 10.32^{+0.29}_{-0.24}(\text{scales}) \pm 0.27(\text{PDF} + \alpha_{\mathrm{s}})\,\text{pb} = 10.32^{+0.40}_{-0.36}(\text{total})\,\text{pb}$, calculated at NLO in QCD with HATHOR 2.1 [51, 52], where the uncertainties due to PDFs and α_{s} were calculated using the PDF4LHC prescription [53] with the MSTW2008NLO 68% CL [54, 55], CT10NLO [56] and NNPDF2.3NLO [35] PDF sets, and were added in quadrature to the effect of the scale uncertainty, defined by taking the envelope of the cross-section values obtained by independently varying the renormalisation and factorisation scales upwards and downwards by a factor of 2 while preventing the two scales from differing by more than a factor of 2. For $t\bar{t}$ production, the predicted cross-section of 832^{+40}_{-46} pb is used, calculated at next-to-next-to-leading order (NNLO) in QCD including the resummation of next-to-next-to-leading logarithmic (NNLL) soft-gluon terms with TOP++ 2.0 [57–63], where the uncertainty accounts for the effect of the PDF and α_{s} uncertainties calculated using the PDF4LHC15 prescription [53] with the MSTW2008NNLO [54, 55], CT10NNLO [56, 64] and NNPDF2.3LO [35] PDF sets, summed in quadrature with the effect of the scale uncertainty. The t-channel single-top-quark cross-section is 217^{+9}_{-8} pb, calculated at NLO in QCD with HATHOR 2.1 [51, 52], where the uncertainty accounts for the effect of the PDF and α_{s} uncertainties calculated using the PDF4LHC15 prescription with the MSTW2008NLO 68% CL, CT10NLO, and NNPDF2.3NLO PDF sets, summed in quadrature with the effect of the scale uncertainty. The tW cross-section is calculated at NLO in QCD with NNLL soft-gluon corrections [65, 66], giving a value of 71.7 ± 3.8 pb, where the uncertainty accounts for the effect of the PDF uncertainty calculated using the MSTW2008NNLO 90% CL PDF set, summed in quadrature with the effect of the scale uncertainty. These predicted cross-sections for top-quark processes are calculated for a top-quark mass of $m_t = 172.5$ GeV. The V+jets MC samples are normalised to cross-sections predicted at NNLO in QCD [67]: 60.2 nb for $W(\to \ell\nu_\ell)$ + jets and 6.32 nb for $Z(\to \ell^+\ell^-)$ + jets, calculated using the FEWZ program [68] with the MSTW2008NNLO PDF set. The diboson MC samples are normalised to the cross-section predicted by the SHERPA 2.2.1 [41] generator.

To model the instrumental background from fake and non-prompt electrons (cf. section 5), dijet events were simulated using PYTHIA 8.186 with the A14 tune and the NNPDF2.3LO PDF sets, and using the EVTGEN 1.2.0 program to model the decays of bottom and charm hadrons. Here, $2 \to 2$ QCD processes were generated, including multijet, $qg \to q\gamma$, $q\bar{q} \to g\gamma$, electroweak (W/Z) and $t\bar{t}$ production processes. This simulated sample was filtered at generator level to enrich the sample with jets which are likely to resemble electron signatures in the detector: events are kept if particles (excluding neutrinos and muons) deposit at least 17 GeV of energy into a square area $\eta \times \phi = 0.1 \times 0.1$, mimicking the highly localised energy deposits characteristic of electrons.

4 Event reconstruction and selection

Events are required to have at least one primary vertex with two or more tracks with $p_{\mathrm{T}} > 0.5$ GeV. If more than one vertex is found, the hard-scattering primary vertex is selected as the one with the highest sum of squared transverse momenta of associated tracks [69].

JHEP06(2023)191

Events were recorded using single-lepton triggers with either a low p_{T} threshold and a lepton isolation requirement, or a higher threshold but a looser identification criterion and without any isolation requirement. The lowest p_{T} threshold in the single-muon trigger was 20 (26) GeV [70] for data taken in 2015 (2016–2018), while in the single-electron trigger it was 24 (26) GeV [71].

Electrons are reconstructed from tracks in the inner tracking detector (ID) associated with topological clusters of energy depositions in the calorimeter [72] and are required to have $p_{\mathrm{T}} > 10\,\mathrm{GeV}$ and $|\eta| < 2.47$. Candidates in the calorimeter barrel–endcap transition region ($1.37 < |\eta| < 1.52$) are excluded. Electrons must satisfy the *Medium* likelihood identification criterion. Muon candidates are identified by matching ID tracks to full tracks or track segments reconstructed in the muon spectrometer, using the *Loose* identification criterion [73]. Muons are required to have $p_{\mathrm{T}} > 10\,\mathrm{GeV}$ and $|\eta| < 2.5$. Lepton tracks must match the primary vertex of the event, i.e. they have to satisfy $|z_0 \sin(\theta)| < 0.5$ mm and $|d_0/\sigma(d_0)| < 5\,(3)$ for electrons (muons), where z_0 is the longitudinal impact parameter relative to the primary vertex and d_0 (with uncertainty $\sigma(d_0)$) is the transverse impact parameter relative to the beam line.

Jets are reconstructed from noise-suppressed topological clusters of calorimeter energy depositions [74] calibrated at the electromagnetic scale [75], using the anti-k_t [76, 77] algorithm with a radius parameter of 0.4. The average energy contribution from pile-up is subtracted according to the jet area and jets are calibrated as described in ref. [75] with a series of simulation-based corrections and in situ techniques. Jets are required to satisfy $p_{\mathrm{T}} > 20\,\mathrm{GeV}$ and $|\eta| < 4.5$. The effect of pile-up is reduced by a so-called jet vertex tagger (JVT) algorithm, applied on jets with $p_{\mathrm{T}} < 120\,\mathrm{GeV}$ and $|\eta| < 2.5$, that uses tracking information to reject calorimeter-based jets that are not consistent with originating from the primary vertex [78].

Jets containing b-hadrons are b-tagged in the $|\eta| < 2.5$ range corresponding to the tracker acceptance, with the MV2c10 multivariate algorithm [79], which combines information about the transverse impact parameters of displaced tracks and the topological properties of secondary and tertiary decay vertices reconstructed within the jet. In this analysis, two working points are used, defined by different thresholds for the MV2c10 discriminant, and corresponding to 85% and 77% efficiencies for b-jets with $p_{\mathrm{T}} > 20\,\mathrm{GeV}$ as determined in simulated $t\bar{t}$ events. The corresponding rejection rate is 2.7 (4.9) for c-jets (containing c-hadrons and no b-hadrons), and 25 (110) for light-jets (containing no c- or b-hadrons), for the 85% (77%) efficiency working point. Correction factors are applied to the simulated events to compensate for differences between data and simulation in the b-tagging efficiency for b-, c-, and light-jets [79–81].

An overlap removal procedure is applied to prevent double-counting of objects. The closest jet within $\Delta R_y = \sqrt{(\Delta y)^2 + (\Delta\phi)^2} = 0.2$ of a selected electron is removed. If the nearest jet surviving that selection is within $\Delta R_y = 0.4$ of the electron, the electron is discarded. Muons are usually removed if they are separated from the nearest jet by $\Delta R_y < 0.4$, since this reduces the background from heavy-flavour decays inside jets. However, if this jet has fewer than three associated tracks, the muon is kept and the jet is removed instead; this avoids an inefficiency for high-energy muons undergoing significant energy loss in the calorimeter.

JHEP06(2023)191

The missing transverse momentum (with magnitude $E_{\mathrm{T}}^{\mathrm{miss}}$) is reconstructed as the negative vector sum of the p_{T} of all the selected electrons, muons, and jets described above, with an extra 'soft term' built from additional tracks associated with the primary vertex, to make it resilient to pile-up contamination [82].

Events are required to have exactly one lepton with $p_{\mathrm{T}} > 30\,\mathrm{GeV}$, and at least two jets with $p_{\mathrm{T}} > 25\,\mathrm{GeV}$ and $|\eta| < 2.5$. The selected lepton is required to match a corresponding object at trigger level. More stringent identification and isolation criteria are applied to increase background rejection: events are kept if the selected electron (muon) satisfies the *Tight* (*Medium*) identification and the *Gradient* [72, 83] isolation criteria. To reduce the contribution of multijet production, which is dominant at low transverse momentum and low transverse mass of the W boson[3] (denoted by m_{T}^{W}), events are required to have $E_{\mathrm{T}}^{\mathrm{miss}} > 35\,\mathrm{GeV}$ and $m_{\mathrm{T}}^{W} > 30\,\mathrm{GeV}$. Events are categorised into four non-overlapping analysis regions, using additional selection criteria described in the following.

The signal region (SR) targets the s-channel single-top signal topology and is used to perform the statistical analysis presented in section 8. In the SR, events contain exactly two jets with $p_{\mathrm{T}} > 30\,\mathrm{GeV}$ and $|\eta| < 2.5$, both b-tagged using the 77% efficiency working point, and at least one of them is required to have $p_{\mathrm{T}} > 40\,\mathrm{GeV}$. In order to reduce the contamination from the dilepton channel of $t\bar{t}$ production (see section 5), events are rejected if they contain additional leptons with $10\,\mathrm{GeV} < p_{\mathrm{T}} < 30\,\mathrm{GeV}$, regardless the more stringent identification and isolation criteria described in the previous paragraph. To reduce the contamination from t-channel single-top production, and from the semileptonic channel of $t\bar{t}$ events, events are rejected if they contain additional jets with $20\,\mathrm{GeV} < p_{\mathrm{T}} < 30\,\mathrm{GeV}$ or with $2.5 < |\eta| < 4.5$.

The $W+$jets validation region ($W+$jets VR) is enriched in $W+$jets events by using a less stringent b-tagging requirement, and is used to assess the modelling of the $W+$jets background (cf. section 5). In the $W+$jets VR, events contain exactly two jets, both with $p_{\mathrm{T}} > 30\,\mathrm{GeV}$ and b-tagged using the 85% efficiency working point, but at least one of these two jets must fail the 77% working point requirement in order to ensure that none of the selected events satisfies the SR requirements. Events are also required to contain no additional lepton with $10\,\mathrm{GeV} < p_{\mathrm{T}} < 30\,\mathrm{GeV}$ regardless the more stringent identification and isolation criteria.

Two validation regions are enriched in $t\bar{t}$ events in order to assess the modelling of this process. In the $t\bar{t}$ 3-jets VR and $t\bar{t}$ 4-jets VR, events are required to have, respectively, exactly three and exactly four jets with $p_{\mathrm{T}} > 25\,\mathrm{GeV}$ and $|\eta| < 2.5$, two of which must be b-tagged using the 77% efficiency working point.

5 Background estimation

Several processes with a final state that is identical or very similar to the single-top s-channel signal are sources of background events for this analysis. The largest background source is $t\bar{t}$ production, which is difficult to distinguish from the signal since such

[3] The transverse mass of the W boson, m_{T}^{W}, is computed from the lepton transverse momentum, p_{T}^{ℓ} and the difference in azimuthal angle, $\Delta\phi(\ell, E_{\mathrm{T}}^{\mathrm{miss}})$ as $m_{\mathrm{T}}^{W} = \sqrt{2E_{\mathrm{T}}^{\mathrm{miss}} p_{\mathrm{T}}^{\ell}[1 - \cos(\Delta\phi(\ell, E_{\mathrm{T}}^{\mathrm{miss}}))]}$.

JHEP06(2023)191

events contain real top-quark decays. In the dileptonic decay mode, $t\bar{t}$ events can mimic the final-state signature of the signal if one of the two leptons is unidentified, whereas the semileptonic decay mode contributes to the selected samples if only two jets are reconstructed. The second most important background source is $W+$jets production. Such events have the same signature as the signal if two jets produced in association with the W boson are b-jets. Furthermore, W-boson production in association with c- or light-jets contributes due to misidentification of such jets as b-jets; this represents 3% of the expected $W+$jets yield. Single top-quark production in the t-channel also leads to a sizeable background contribution, while associated tW production has a smaller event yield. Both $Z+$jets and diboson production are minor background sources. These background processes, as well as the signal, are modelled using MC event samples and normalised to cross-sections predicted in the SM, as described in section 3, before the signal extraction fit described in section 8.

In addition, multijet production contributes to the selected events, when jets, non-prompt leptons from heavy-flavour decays, or electrons from photon conversion, are misidentified as prompt isolated leptons. The modelling of this background in the electron (muon) channel relies on the so-called jet-electron (anti-muon) method described in refs. [84, 85], in which a dedicated simulated (data) event sample is used as a model for the shapes of the different distributions. The normalisation of the multijet background is extracted from data for both channels, using a dedicated fit described in this section. Both normalisations and shapes are later used as input for the signal extraction fit described in section 8.

In the case of the jet-electron model, a dedicated selection is imposed on the MC simulated dijet events sample described in section 3, in order to select the events with jets that are likely to resemble a lepton in the detector. Such jets are required to deposit a large amount of their energy in the electromagnetic calorimeter, and are treated as electrons in the event selection. In order to reduce the uncertainty due to the size of the MC sample, the b-tagging requirements imposed on two of the jets in the event selection described in section 4 are not applied. In the case of the anti-muon model, a dedicated data sample is used. Some of the muon identification criteria, related to the energy loss in the calorimeter, to the longitudinal impact parameter, or to the tracking and calorimeter isolation, are inverted or changed [73, 84], resulting in a sample that is enriched with events containing fake or non-prompt muons from multijet events.

The jet-electron and anti-muon event samples are then used to estimate the multijet background normalisation in a binned maximum-likelihood fit, using variables chosen to provide good separation between the background sources: the $E_{\mathrm{T}}^{\mathrm{miss}}$ distribution in the electron channel, and the m_{T}^{W} distribution in the muon channel. For this purpose, the region definitions are modified in order to increase the number of multijet background events in the selected sample: the requirements on $E_{\mathrm{T}}^{\mathrm{miss}}$ in the electron channel, and on m_{T}^{W} in the muon channel, are not applied. A simultaneous fit of the electron and muon channels is performed in the SR to extract the normalisations of both the jet-electron and anti-muon samples, which are allowed to float freely and independently in the fit. The obtained multijet normalisation is used in the SR as an initial value for the signal extraction fit described

JHEP06(2023)191

in section 8. The normalisation of the $W+$jets contribution is also allowed to float freely in the fit, and so is the normalisation of the top-quark processes. The latter are grouped together in one template where the relative contributions are fixed to their SM predictions, as they show similar $E_{\mathrm{T}}^{\mathrm{miss}}$ and m_{T}^{W} distributions. The normalisation factors extracted for the $W+$jets and top-quark processes in this fit are, however, not used for the signal extraction fit described in section 8. The normalisations of the other processes are fixed to their SM predictions. The fit is repeated in each of the three VRs to extract the multijet normalisation in these regions. In the $W+$jets VR ($t\bar{t}$ 3-jets VR and $t\bar{t}$ 4-jets VR), the normalisation of the $W+$jets contribution (top-quark processes contribution) is allowed to float freely, while the normalisations of the other processes are fixed to their SM predictions. The multijet normalisation obtained in the three VRs is used to validate the modelling of the discriminant, as described in section 6.

Figures 2 and 3 show the $E_{\mathrm{T}}^{\mathrm{miss}}$ and m_{T}^{W} distributions in the electron and muon channels respectively, after the fit of the multijet background in each region. In these distributions, the uncertainties in the background normalisations described in section 7 are included, as well as 6 % and 40 % uncertainties in the $t\bar{t}$ and $W+$jets background normalisations, motivated respectively by the uncertainty in the $t\bar{t}$ cross-section prediction (cf. section 3) and the value of the $W+$jets normalisation factor extracted in the fit – while they are eventually treated as unconstrained parameters in the statistical analysis of the signal cross-section (cf. section 8). The predictions after the fit are in agreement with the data, given the statistical and systematic uncertainties. The trends seen at low $E_{\mathrm{T}}^{\mathrm{miss}}$ or m_{T}^{W} values for the best fit distribution would not impact the signal extraction fit, for which the $E_{\mathrm{T}}^{\mathrm{miss}} > 35\,\mathrm{GeV}$ and $m_{\mathrm{T}}^{W} > 30\,\mathrm{GeV}$ requirements are applied (cf. section 4). Furthermore, the trends seen at high $E_{\mathrm{T}}^{\mathrm{miss}}$ or m_{T}^{W} values are consistent with the mismodelling, seen in other analyses [86], of $t\bar{t}$ events by MC generators at NLO in QCD, which predict harder top-quark p_{T} spectra than observed in data, and which are typically covered by the relevant $t\bar{t}$ modelling systematic uncertainties described in section 7.

6 Matrix element method

The matrix element method (MEM) [16, 17] directly uses theoretical calculations to compute a per-event signal probability. This technique was used for the observation of single top-quark production in proton–antiproton collisions at the Tevatron [3, 4, 87–89], and in finding evidence of single top-quark s-channel production in proton–proton collisions in ATLAS [15]. The discrimination between signal and background is based on the computation of likelihood values $\mathcal{P}(X \mid H_{\mathrm{proc}})$ for the hypothesis that a measured event with final state X defined by the presence of certain reconstructed objects, is of a certain process type H_{proc}. The likelihoods can be computed by means of the factorisation theorem from the corresponding partonic cross-sections of the hard scattering process, as follows:

$$\mathcal{P}(X \mid H_{\mathrm{proc}}) = \int \mathrm{d}\Phi \, \frac{1}{\sigma_{H_{\mathrm{proc}}}} \frac{\mathrm{d}\sigma_{H_{\mathrm{proc}}}}{\mathrm{d}\Phi} T_{H_{\mathrm{proc}}}(X \mid \Phi) \; .$$

The normalised fully differential cross-section $(1/\sigma_{H_{\mathrm{proc}}})(\mathrm{d}\sigma_{H_{\mathrm{proc}}}/\mathrm{d}\Phi)$ gives the probability density for a scattering process H_{proc} to lead to a parton-level final state Φ as a function of

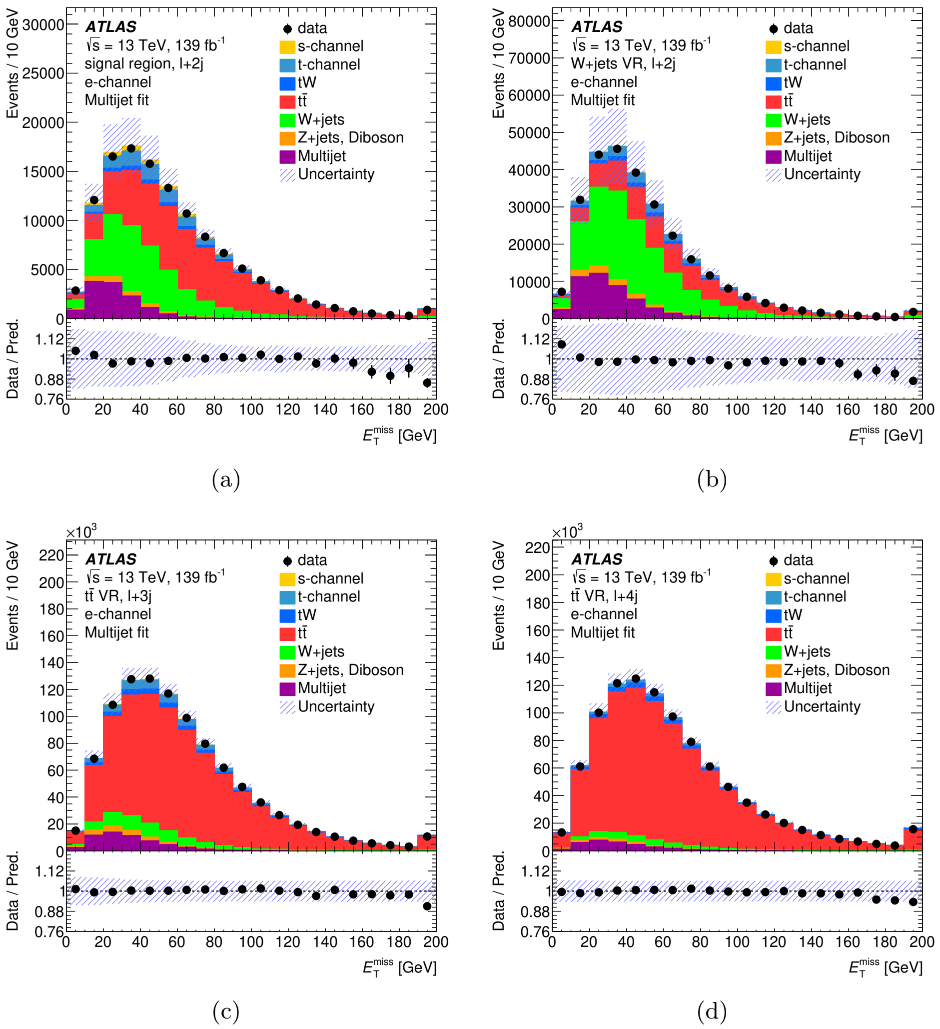

Figure 2. Distribution of $E_{\mathrm{T}}^{\mathrm{miss}}$ after the fit of the multijet backgrounds, in the electron channel, in the (a) signal region, (b) W+jets VR, (c) $t\bar{t}$ 3-jets VR, and (d) $t\bar{t}$ 4-jets VR without applying the requirement on $E_{\mathrm{T}}^{\mathrm{miss}}$. Simulated events are normalised to the expected number of events given the integrated luminosity, after applying the normalisation factors obtained in the multijet fit. The last bin includes the overflow. The uncertainty bands indicate the simulation's statistical uncertainty, the normalisation uncertainties for different processes (40% for W+jets production, 30% for multijet background and 6% for top-quark processes) and the multijet background shape uncertainty in each bin, summed in quadrature. The lower panels show the ratio of the data to the prediction.

the four-momenta of all outgoing particles. The mapping between the measured final state X and the parton-level state Φ is implemented by transfer functions $T_{H_{\mathrm{proc}}}(X \mid \Phi)$ which take into account the detector energy-resolution functions, the reconstruction efficiencies for the electron, the muon and the jets, and the b-tagging efficiencies, as a function of the parton-level transverse momenta and pseudorapidities, and the efficiency of the $E_{\mathrm{T}}^{\mathrm{miss}}$ selection as a function of the neutrino transverse momentum. The permutations between

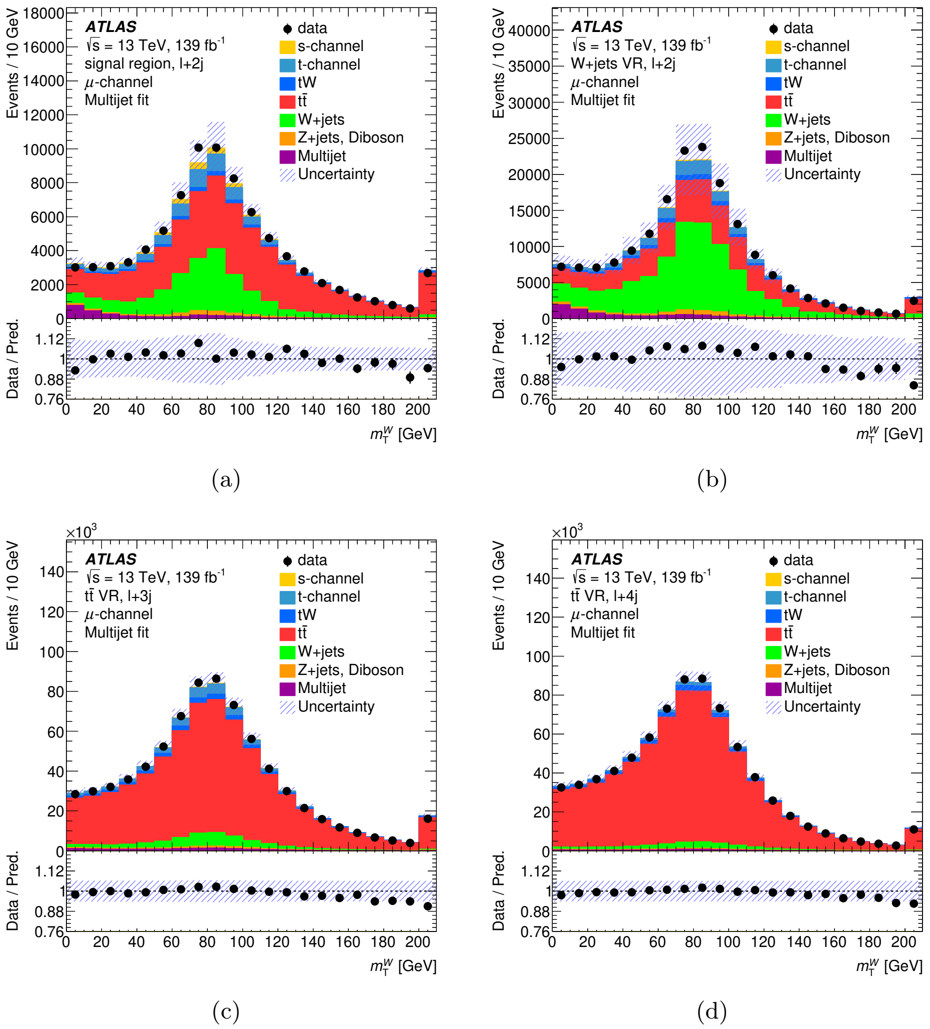

Figure 3. Distribution of m_T^W after the fit of the multijet backgrounds, in the muon channel, in the (a) signal region, (b) $W+$jets VR, (c) $t\bar{t}$ 3-jets VR, and (d) $t\bar{t}$ 4-jets VR without applying the requirement on m_T^W. Simulated events are normalised to the expected number of events given the integrated luminosity, after applying the normalisation factors obtained in the multijet fit. The last bin includes the overflow. The uncertainty bands indicate the simulation's statistical uncertainty, the normalisation uncertainties for different processes (40% for $W+$jets production, 30% for multijet background and 6% for top-quark processes) and the multijet background shape uncertainty in each bin, summed in quadrature. The lower panels show the ratio of the data to the prediction.

the partons and the reconstructed objects are taken into account by summing over the possible configurations which contribute to the differential cross-section [87, 89].

The phase-space integration of the differential partonic cross-sections is performed by using the Monte Carlo integration algorithm Vegas [90] from the Cuba program library [91]. The required PDF sets are taken from the LHAPDF5 package [92], while the computation of the scattering amplitudes is based on code from the MCFM program [93]. The functional forms and parameterisations of the ATLAS detector resolutions used for the transfer

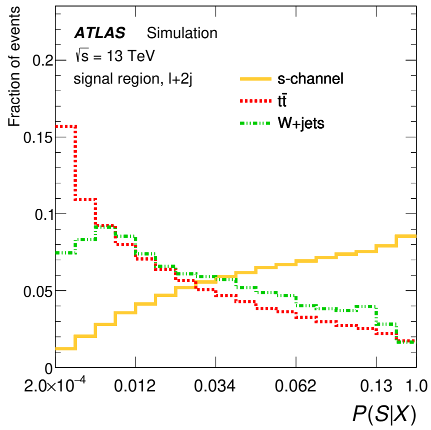

Figure 4. Expected distributions of the MEM discriminant $P(S|X)$ in the SR, for the s-channel single-top signal, and for the $t\bar{t}$ and $W+$jets backgrounds, for MEM discriminant values larger than 2.0×10^{-4}. Each distribution is normalised to unity. The binning is the same as the optimised binning used in the signal extraction fit, resulting in a non-linear horizontal scale.

functions are those used in the KLFitter kinematic fit framework [94, 95]. The parameters are derived from event samples produced using the ATLAS detector simulation.

In total, eight different processes, all having at least one charged lepton, one neutrino, and two quarks in the final state, are considered for the computation of the likelihood values: two processes for the s-channel single-top-quark signal (one with two final-state partons corresponding to the b-quarks in the LO diagram, and one with three final-state partons in which a real radiation correction is included), one process for the t-channel single-top-quark background (which is modelled in the four-flavour scheme only), two processes for $t\bar{t}$ production (for the semileptonic and dileptonic final states, which are evaluated separately), and three processes for the remaining W-boson background production (one process with two associated light-jets, one process with one light-jet and one c-jet, and one process with two b-jets). The scattering matrix elements for all considered processes are calculated using LO amplitudes.

From the likelihood values of these processes the probability $P(S\,|X)$ for a measured event X to be a signal event S can be computed with Bayes' theorem by:

$$P(S \mid X) = \frac{\sum_i P(S_i)\, \mathcal{P}(X \mid S_i)}{\sum_i P(S_i)\, \mathcal{P}(X \mid S_i) + \sum_j P(B_j)\, \mathcal{P}(X \mid B_j)}\,.$$

Here, S_i and B_j denote all signal and background processes that are considered. The a priori probabilities $P(S_i)$ and $P(B_j)$ are taken to be the expected event fractions from the various processes contributing to the signal region, as obtained from Monte Carlo simulations; variations of these factors were observed to have negligible impact on the sensitivity. The final state X of the measured events have the SR topology: one electron or muon, two b-tagged jets, and missing transverse momentum. The value of $P(S\,|X)$ is taken as the discriminant in the signal extraction. Figure 4 shows its expected distribution for the s-channel single-top-quark signal and for the $t\bar{t}$ and $W+$jets background contributions

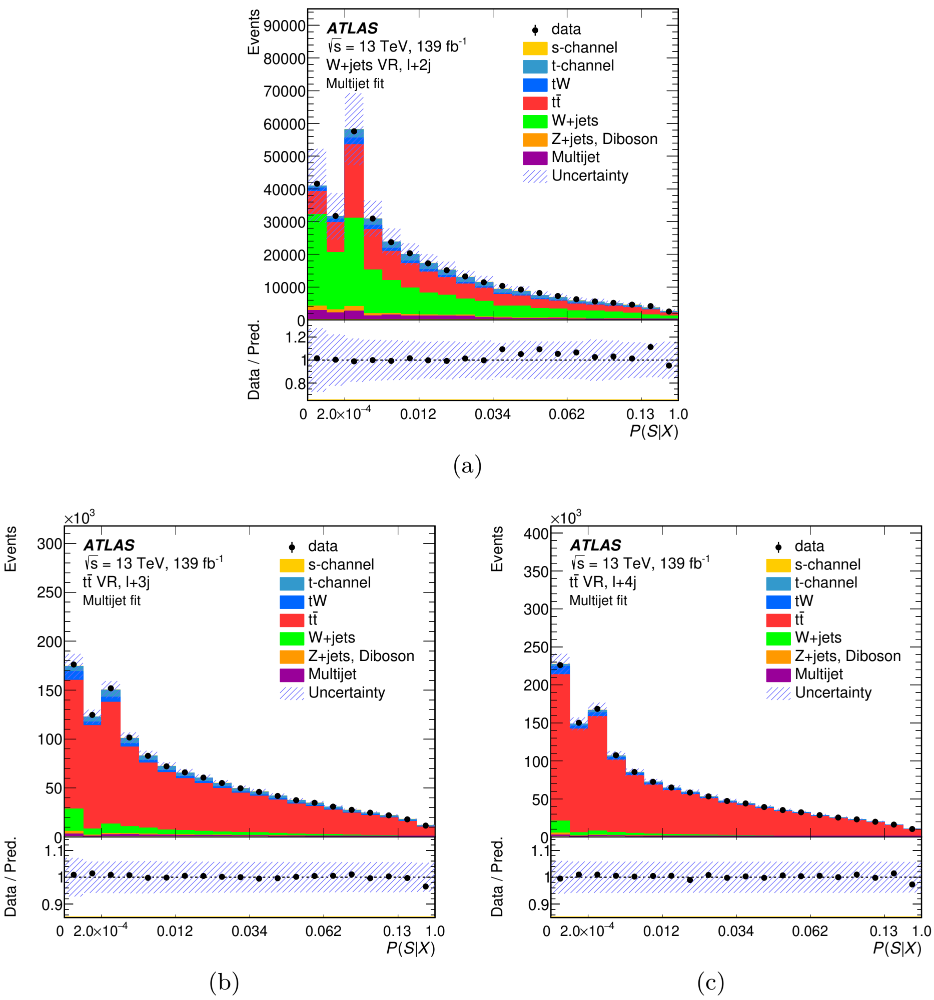

Figure 5. Distributions of the MEM discriminant $P(S|X)$ in the (a) W+jets VR, (b) $t\bar{t}$ 3-jets VR, and (c) $t\bar{t}$ 4-jets VR. Simulated events are normalised to the expected number of events given the integrated luminosity, after applying the normalisation factors obtained in the multijet fit presented in section 5. The uncertainty bands indicate the simulation's statistical uncertainty and the normalisation uncertainties for the various processes in each bin, summed in quadrature. The ratio of the observed number to the predicted number of events in each bin is shown in the lower panel, with different vertical axis ranges. The binning is the same as the optimised binning used in the signal extraction fit described in section 8, resulting in a non-linear horizontal scale.

in the SR, with the same binning and range as used for the signal extraction described in section 8.

In order to validate the s-channel MEM discriminant $P(S|X)$, it is computed in the three validation regions. For the $t\bar{t}$ VRs, in which events with three or four jets are selected, only the two b-tagged jets are considered for the MEM discriminant computation, since most of the considered processes have only two outgoing partons. For the jet-electron sample, in which the b-tagging requirement is not applied (cf. section 5), only the two leading jets are considered. Figure 5 compares the discriminant distribution in data with that in simulation for the three VRs, using the same optimised binning as used for the signal extraction fit in the SR described in section 8. In these distributions, produced prior to the signal extraction fit, the uncertainty band includes the normalisation uncertainties of all processes, including the signal and the $t\bar{t}$ and $W+$jets backgrounds, as well as the simulation's statistical uncertainty. Good modelling is observed in the three validation regions.

7 Systematic uncertainties

Systematic uncertainties affect the signal acceptance and the background normalisations. Furthermore, most of them affect the shape of the MEM discriminant distribution because they affect the four-momenta of the reconstructed objects, or their efficiencies. Uncertainties related to the detector and to the modelling of the signal and background processes are taken into account. In the statistical analysis, an independent nuisance parameter is assigned to each source of systematic uncertainty. Several of the systematic uncertainties are decomposed into components from multiple independent sources.

The uncertainty in the combined 2015–2018 integrated luminosity is 1.7% [96], obtained using the LUCID-2 detector [97] for the primary luminosity measurement. An uncertainty associated with the modelling of pile-up in the simulation is included to cover the difference between the predicted and measured inelastic cross-section values [98].

The jet energy scale uncertainty is derived by combining information from test-beam data, LHC collision data and simulation, and the jet energy resolution uncertainty is obtained by combining dijet p_{T}-balance measurements and simulation [75]. Additional considerations related to jet flavour, pile-up corrections, η dependence and high-p_{T} jets are included. A total of 31 independent contributions are considered for the jet energy scale uncertainty, and 9 for the jet energy resolution uncertainty. The efficiency of the JVT algorithm to identify and remove jets from pile-up is measured with $Z \to \mu^+\mu^-$ events in data using techniques similar to those used in ref. [78].

The efficiency to correctly tag b-jets is measured using dileptonic $t\bar{t}$ events [79]. The mis-tag rate for c-jets is measured using semileptonic $t\bar{t}$ events, exploiting the c-jets from the hadronic W-boson decays using techniques similar to those in ref. [80]. The mis-tag rate for light-jets is measured using a negative-tag method, similar to that in ref. [81], applied to $Z+$jets events. Uncertainties on this efficiency and these mis-tag rates are due to reconstructed object calibrations and to the modelling of the different processes, and are decomposed into sets of uncorrelated sources of uncertainty: 45, 20, and 20 components for b-, c- and light-jets, respectively.

Uncertainties associated with leptons arise from the trigger, reconstruction, identification, and isolation, as well as the lepton momentum scale and resolution. Efficiencies are measured, and calibrations of the scale and resolution are performed, using leptons in $Z \to \ell^+\ell^-$ and $J/\psi \to \ell^+\ell^-$ events [72, 83]. Systematic uncertainties in these measurements account for 22 independent sources.

All uncertainties related to the energy scales or resolution of the reconstructed objects are propagated to the calculation of the missing transverse momentum. Three additional uncertainties associated with the scale and resolution of the soft term are also included.

The modelling of the cross-section and acceptance of the two dominant backgrounds, $t\bar{t}$ and $W+$jets production, is affected by several systematic uncertainties. Therefore, the normalisations of these processes are measured in the signal extraction fit (cf. section 8), and no constraints are placed on these two freely floating parameters. For single-top t-channel and tW production, uncertainties in the theoretical cross-sections of 4 % and 5 %, respectively, are propagated to the statistical analysis. For Z+jets and diboson processes, an uncertainty of 60 % is considered, including ±5% for the inclusive cross-section summed in quadrature with ±24% per additional jet and ±50% for the heavy-flavour component [15, 99, 100]. Finally, an uncertainty of 30 % is assigned to the normalisation of the multijet background, motivated by the change in the multijet normalisation when altering various settings in the multijet fit described in section 5, or by comparisons with other methods of estimating this background, as used in previous analyses [84, 85].

Uncertainties due to the modelling of the different processes are taken into account. For each of the single-top s-channel, t-channel and tW processes, and the $t\bar{t}$ process, four sources related to the modelling of initial- and final-state radiation (ISR/FSR) are considered: two independent sources estimated by separately varying the renormalisation and factorisation scales in the ME generator by factors of 0.5 and 2, one source estimated by varying the renormalisation scale for QCD emission in the initial-state radiation in Pythia 8 (corresponding to the Var3c variation of the A14 tune [34]), and one source estimated by halving and doubling the renormalisation scale for QCD emission in the final-state radiation in Pythia 8. One additional source is also estimated for each of these four top-quark processes to account for the parton shower and hadronisation model, by comparing the nominal Powheg Box + Pythia 8 MC sample with a Powheg Box + Herwig 7.04 sample. The uncertainty associated with the algorithm removing the overlap between tW and $t\bar{t}$ production at NLO [37] is assessed by comparing the nominal Powheg Box + Pythia 8 tW sample produced using the diagram removal scheme with an alternative sample produced with the same generator but using the diagram subtraction scheme. For the dominant $t\bar{t}$ background, two additional sources are considered: one source related to soft gluon resummation is estimated by setting the h_{damp} parameter to $3.0 \cdot m_t$, instead of the nominal $1.5 \cdot m_t$, in the Powheg Box + Pythia 8 $t\bar{t}$ MC sample, and one source related to the matching of the ME to the parton shower is estimated by comparing the nominal Powheg Box + Pythia 8 $t\bar{t}$ MC sample with a MadGraph5_aMC@NLO + Pythia 8 sample. One source of uncertainty related to the shape of the $W+$jets background is evaluated by using the envelope of the independent variations of the renormalisation and factorisation scales in the ME of the $W+$jets MC sample. Two sources of uncertainty affecting the shape of the multijet background are considered, one for the electron channel and one for the muon channel. These two sources are estimated by varying the criteria related to the fraction of energy deposited in the electromagnetic calorimeter for the jet-electron model, and to the tracking isolation in the anti-muon model, respectively (cf. section 5). All these modelling uncertainties may affect both the shape of the MEM discriminant and the normalisation of each process, except for $t\bar{t}$ and $W+$jets, for which the normalisation is extracted in the fit.

The choice of PDFs affects the modelling of top-quark processes, and these uncertainties are evaluated using the PDF4LHC15 combined PDF error sets [53], which contain 30 symmetric eigenvectors. Four independent sets of 30 uncertainty sources are considered, one for each process. For single-top t-channel production, the PDF4LHC15_nlo_nf4_30 set is used, while for single-top s-channel and tW production, and $t\bar{t}$ production, the PDF4LHC15_nlo_30 set is used.

8 Signal extraction

The single-top-quark s-channel production cross-section is measured by means of a binned profile maximum-likelihood fit of the MEM discriminant in the signal region. The binning of the MEM discriminant is optimised in the signal region using the procedure described in ref. [101], in order to maximise the expected sensitivity while keeping the total statistical uncertainty of the predicted number of events in each bin at a level adjusted to avoid biases due to fluctuations. This results in bins of unequal width, with wider bins in regions with a large signal contribution, while preserving a sufficiently large number of background events in each bin. In this paper, MEM discriminant distributions are presented with a non-linear horizontal scale, in such a way that the histogram bins appear to have a constant width. Values of $P(S|X)$ lower than 2.0×10^{-4} are not taken into account for the signal extraction because of the very low signal-to-background ratio in this range; this rejects 21% (18%) of the expected $t\bar{t}$ (W+jets) background events, while the expected signal yield is reduced by less than 1%. The electron and muon channels, which have similar sensitivity to the signal, are merged regardless of the lepton charge or flavour or of the various data-taking periods of the LHC, while preserving correlations of the later described nuisance parameters associated to systematic uncertainties, in order to measure the combined production cross-section of single top quarks and top antiquarks.

The binned likelihood function $\mathcal{L}(\mu, \theta)$ used in the fit consists of a product of Poisson probability terms over the signal region histogram bins. The likelihood function depends on the signal strength μ, defined as $\mu = \sigma/\sigma^{\mathrm{SM}}$, where σ is the observed signal production cross-section, and on a set of nuisance parameters θ, which characterise the effects of systematic uncertainties in the signal and background predictions. They are implemented in the likelihood function as Gaussian priors, with the exception of the unconstrained normalisation factors for the $t\bar{t}$ and W+jets backgrounds. The statistical uncertainty in the predictions, which incorporates the statistical uncertainty arising from the limited number of simulated events, is included in the likelihood function in the form of additional nuisance parameters, one for each of the considered bins, and constrained by Poisson priors. The test statistic t_μ is defined as the profile likelihood ratio: $t_\mu = -2\ln(\mathcal{L}(\mu, \hat{\hat{\theta}}_\mu)/\mathcal{L}(\hat{\mu}, \hat{\theta}))$, where $\hat{\mu}$ and $\hat{\theta}$ are the values of the parameters which maximise the likelihood function, and $\hat{\hat{\theta}}_\mu$ are the values of the nuisance parameters which maximise the likelihood function for a given value of μ [102]. This test statistic, implemented in a framework based on RooStats [103, 104] and HistFactory [105], is used to assess the compatibility of the observed data with the background-only hypothesis, and to make statistical inferences about μ.

9 Results

A comparison of the MEM discriminant distributions in data and simulation is shown in figure 6, before and after the fit to data. The uncertainty in the total prediction before

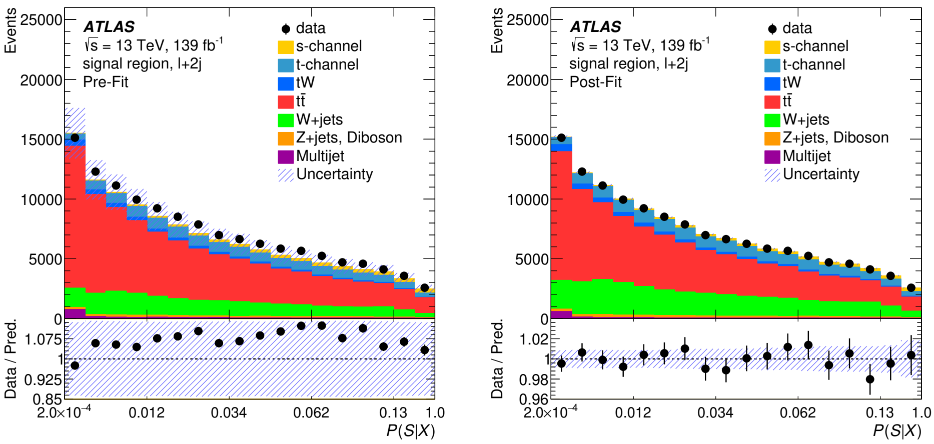

(a) (b)

Figure 6. Distributions of the MEM discriminant $P(S|X)$ in the SR (a) before and (b) after the fit to data, for MEM discriminant values larger than 2.0×10^{-4}. The lower panels show the ratio of the data to the prediction, with different vertical axis ranges. The uncertainty bands indicate the total uncertainties and their correlations in each bin. The uncertainties in the $t\bar{t}$ and $W+$jets normalisation factors, as well as in the s-channel signal cross-section, are not defined pre-fit and therefore only included in the post-fit uncertainties in (b). The binning is the same as the optimised binning used in the fit, resulting in a non-linear horizontal scale.

the fit in figure 6(a) is dominated by signal modelling, the jet energy resolution and scale, ISR/FSR in top-quark processes, and $t\bar{t}$ modelling uncertainties. The distribution after the fit in figure 6(b) shows good agreement within the total uncertainty band, and the global goodness of fit calculated using the saturated model [106] is 10.3%. The measured distribution of the MEM discriminant for the signal contribution is shown in figure 7, and is compared with the data after the subtraction of all background contributions. The expected event yields for the different processes, before and after the fit, are shown in table 1, together with the observed event yield in data. The measured $t\bar{t}$ and $W+$jets normalisation factors are $0.81^{+0.13}_{-0.12}$ and $1.37^{+0.35}_{-0.31}$, respectively; their correlation is 51%, and their respective correlations with the signal cross-section are 55% and 27%. After the fit, none of the other nuisance parameters is pulled by more than 0.8 standard deviation, constrained to less than 74% of its pre-fit impact on the cross-section by the fit, or has a correlation with the fitted cross-section larger than 33%.

Several tests were performed in order to assess the robustness of this fit, called 'baseline fit' in this paragraph. First, instead of being left unconstrained, the $t\bar{t}$ and $W+$jets normalisations were assigned an uncertainty on their cross-sections. In such case, the nuisance parameters associated to these uncertainties were pulled in the same directions as the normalisation factors in the baseline fit. Second, a fit of the background-only hypothesis to the data was performed, keeping only bins of the discriminant distribution in which the expected signal-to-background ratio does not exceed 5%. In such a fit, the $t\bar{t}$ and $W+$jets normalisation factors were pulled by values compatible to those obtained in the baseline fit. Furthermore, the post-fit nuisance parameters of this background-only fit were propagated

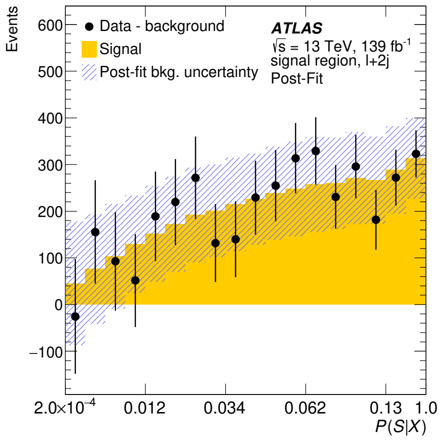

Figure 7. Distribution of the MEM discriminant $P(S|X)$ in the SR after the fit to data, for MEM discriminant values larger than 2.0×10^{-4}, after subtraction of all backgrounds. The fitted distribution for the simulation of the signal is shown together with the post-fit uncertainty in the backgrounds. The binning is the same as the optimised binning used in the fit, resulting in a non-linear horizontal scale.

Process	Event yield	
	Pre-fit	Post-fit
s-channel	$4\,200 \pm 710$	$3\,700 \pm 1\,100$
t-channel	$13\,000 \pm 2\,000$	$15\,000 \pm 2\,300$
tW	$3\,680 \pm 970$	$4\,250 \pm 1\,100$
$t\bar{t}$	$76\,000 \pm 12\,000$	$70\,600 \pm 4\,200$
$W+$jets	$21\,500 \pm 2\,900$	$32\,200 \pm 5\,000$
$Z+$jets, VV	$2\,400 \pm 1\,400$	$2\,900 \pm 1\,600$
Multijet	$2\,150 \pm 650$	$1\,700 \pm 540$
Total	$123\,000 \pm 17\,000$	$130\,310 \pm 620$
Data	130 310	

Table 1. Pre-fit and post-fit event yields in the SR, for MEM discriminant values larger than 2.0×10^{-4}. The central value of the event yield for each process is calculated by summing the values of the discriminant bin contents, using the nominal expected yield for the pre-fit value, and the best-fit estimate for the post-fit value. The error includes statistical and systematic uncertainties summed in quadrature. All sources of systematic uncertainties are included, taking into account correlations and anti-correlations in the post-fit case. The uncertainties in the $t\bar{t}$ and $W+$jets normalisation factors, as well as in the s-channel signal cross-section, are not defined pre-fit and therefore only included in the post-fit uncertainties.

to the signal and background MC samples, with signal cross-section set to its prediction from theory, in order to build a 'realistic' pseudo-data set. A signal-plus-background fit to this pseudo-data set was then performed, and the measured cross-section was compatible with the predicted cross-section. Finally, the linearity of the statistical model was checked, by performing fits to pseudo-data sets produced from the nominal predictions (Asimov datasets), where the expected signal cross-section was increased or decreased. In such fits, the measured and expected cross-sections were in agreement.

JHEP06(2023)191

Source	$\Delta\sigma/\sigma$ [%]
$t\bar{t}$ normalisation	+24/−17
$t\bar{t}$ shape modelling	+18/−15
ISR/FSR	+13/−11
PS & had.	+12/−10
ME/PS matching	+10/−8
h_{damp}	< 1
s-channel modelling	+18/−8
PS & had.	+18/−8
ISR/FSR	+3/−1
Jet energy resolution	+18/−12
Jet energy scale	+18/−13
MC statistics	+13/−11
Flavour tagging	+12/−10
$W+$jets normalisation	+11/−8
PDFs	+10/−9
$t\bar{t}$	+10/−9
s-channel	±1
t-channel	±1
tW	±1
t-channel modelling	±6
PS & had.	±5
ISR/FSR	±4
$W+$jets $\mu_{\text{r}}/\mu_{\text{f}}$ shape	+6/−5
Normalisation of other processes	+6/−5
Pile-up	+5/−3
Luminosity	+4/−3
tW modelling	+1/−2
PS & had.	±1
$t\bar{t}$ overlap	±1
ISR/FSR	±1
Missing transverse momentum	±1
Multijet shape modelling	±1
Other detector sources	±1
Systematic uncertainties	+42/−34
Statistical uncertainty	±8
Total	+42/−35

Table 2. Observed impact of the different sources of uncertainty on the measured s-channel signal cross-section, grouped by categories. The impact of each category is obtained by repeating the fit after having fixed the set of nuisance parameters corresponding to that category, subtracting the square of the resulting uncertainty from the square of the uncertainty found in the full fit, and calculating the square root. The statistical uncertainty is obtained by repeating the fit after having fixed all nuisance parameters, including the $t\bar{t}$ and $W+$jets normalisation factors. 'PS & had.' refers to the parton shower and hadronisation model, 'ME/PS matching' to the matching of the ME to the parton shower, and '$t\bar{t}$ overlap' to the algorithm removing the overlap between tW and $t\bar{t}$ production at NLO, as described in section 7.

The measured cross-section is $\sigma = 8.2 \pm 0.6\ (\text{stat.})^{+3.4}_{-2.8}\ (\text{syst.})\ \text{pb} = 8.2^{+3.5}_{-2.9}\ (\text{total})\ \text{pb}$, which is compatible with the SM prediction of $\sigma^{\text{SM}} = 10.32^{+0.40}_{-0.36}\ \text{pb}$. A summary of the main sources of uncertainty is presented in table 2. The largest contribution arises from the $t\bar{t}$ normalisation. Uncertainties in the jet energy scale and resolution, and in the signal generator modelling, also play an important role, followed by the modelling of ISR/FSR in top-quark processes, the statistical uncertainty of the MC predictions, the $t\bar{t}$ generator modelling uncertainties, and the flavour-tagging uncertainties. The observed signal significance is 3.3 standard deviations above the background-only hypothesis, while the expected significance is 3.9 standard deviations.

10 Conclusion

A measurement of the s-channel single-top-quark production cross-section in pp collisions at a centre-of-mass energy of 13 TeV recorded by the ATLAS detector at the LHC is presented. The analysis was performed using data collected in 2015–2018 corresponding to an integrated luminosity of $139\,\mathrm{fb}^{-1}$. The selected events contain one electron or muon, two jets which are both b-tagged, and missing transverse momentum. The matrix element method was used to obtain a discriminant to separate the signal from the background events, and the signal was extracted using a profile likelihood fit. The measured signal cross-section, combining top-quark and top-antiquark production, is $\sigma = 8.2^{+3.5}_{-2.9}\,\mathrm{pb}$, in agreement with the SM prediction of $\sigma^{\mathrm{SM}} = 10.3 \pm 0.4\,\mathrm{pb}$. The observed (expected) signal significance is 3.3 (3.9) standard deviations above the background-only hypothesis. This result provides a measurement of the cross-section of this process at a new centre-of-mass energy, which allows the energy dependence of this observable to be probed.

Acknowledgments

We thank CERN for the very successful operation of the LHC, as well as the support staff from our institutions without whom ATLAS could not be operated efficiently.

We acknowledge the support of ANPCyT, Argentina; YerPhI, Armenia; ARC, Australia; BMWFW and FWF, Austria; ANAS, Azerbaijan; CNPq and FAPESP, Brazil; NSERC, NRC and CFI, Canada; CERN; ANID, Chile; CAS, MOST and NSFC, China; Minciencias, Colombia; MEYS CR, Czech Republic; DNRF and DNSRC, Denmark; IN2P3-CNRS and CEA-DRF/IRFU, France; SRNSFG, Georgia; BMBF, HGF and MPG, Germany; GSRI, Greece; RGC and Hong Kong SAR, China; ISF and Benoziyo Center, Israel; INFN, Italy; MEXT and JSPS, Japan; CNRST, Morocco; NWO, Netherlands; RCN, Norway; MEiN, Poland; FCT, Portugal; MNE/IFA, Romania; MESTD, Serbia; MSSR, Slovakia; ARRS and MIZŠ, Slovenia; DSI/NRF, South Africa; MICINN, Spain; SRC and Wallenberg Foundation, Sweden; SERI, SNSF and Cantons of Bern and Geneva, Switzerland; MOST, Taiwan; TENMAK, Türkiye; STFC, United Kingdom; DOE and NSF, United States of America. In addition, individual groups and members have received support from BCKDF, CANARIE, Compute Canada and CRC, Canada; PRIMUS 21/SCI/017 and UNCE SCI/013, Czech Republic; COST, ERC, ERDF, Horizon 2020 and Marie Skłodowska-Curie Actions, European Union; Investissements d'Avenir Labex, Investissements d'Avenir Idex and ANR, France; DFG and AvH Foundation, Germany; Herakleitos, Thales and Aristeia programmes co-financed by EU-ESF and the Greek NSRF,

JHEP06(2023)191

Greece; BSF-NSF and MINERVA, Israel; Norwegian Financial Mechanism 2014-2021, Norway; NCN and NAWA, Poland; La Caixa Banking Foundation, CERCA Programme Generalitat de Catalunya and PROMETEO and GenT Programmes Generalitat Valenciana, Spain; Göran Gustafssons Stiftelse, Sweden; The Royal Society and Leverhulme Trust, United Kingdom.

The crucial computing support from all WLCG partners is acknowledged gratefully, in particular from CERN, the ATLAS Tier-1 facilities at TRIUMF (Canada), NDGF (Denmark, Norway, Sweden), CC-IN2P3 (France), KIT/GridKA (Germany), INFN-CNAF (Italy), NL-T1 (Netherlands), PIC (Spain), ASGC (Taiwan), RAL (UK) and BNL (USA), the Tier-2 facilities worldwide and large non-WLCG resource providers. Major contributors of computing resources are listed in ref. [107].

References

[1] T.M.P. Tait and C.-P. Yuan, *Single top quark production as a window to physics beyond the standard model*, *Phys. Rev. D* **63** (2000) 014018 [hep-ph/0007298] [INSPIRE].

[2] Q.-H. Cao, J. Wudka and C.-P. Yuan, *Search for new physics via single top production at the LHC*, *Phys. Lett. B* **658** (2007) 50 [arXiv:0704.2809] [INSPIRE].

[3] CDF collaboration, *First observation of electroweak single top quark production*, *Phys. Rev. Lett.* **103** (2009) 092002 [arXiv:0903.0885] [INSPIRE].

[4] D0 collaboration, *Observation of single top quark production*, *Phys. Rev. Lett.* **103** (2009) 092001 [arXiv:0903.0850] [INSPIRE].

[5] CDF and D0 collaborations, *Observation of s-channel production of single top quarks at the Tevatron*, *Phys. Rev. Lett.* **112** (2014) 231803 [arXiv:1402.5126] [INSPIRE].

[6] CMS collaboration, *Measurement of the single-top-quark t-channel cross section in pp collisions at* $\sqrt{s} = 7$ *TeV*, *JHEP* **12** (2012) 035 [arXiv:1209.4533] [INSPIRE].

[7] ATLAS collaboration, *Measurement of the t-channel single top-quark production cross section in pp collisions at* $\sqrt{s} = 7$ *TeV with the ATLAS detector*, *Phys. Lett. B* **717** (2012) 330 [arXiv:1205.3130] [INSPIRE].

[8] CMS collaboration, *Observation of the associated production of a single top quark and a W boson in pp collisions at* $\sqrt{s} = 8$ *TeV*, *Phys. Rev. Lett.* **112** (2014) 231802 [arXiv:1401.2942] [INSPIRE].

[9] ATLAS collaboration, *Measurement of the production cross-section of a single top quark in association with a W boson at* 8 *TeV with the ATLAS experiment*, *JHEP* **01** (2016) 064 [arXiv:1510.03752] [INSPIRE].

[10] CMS collaboration, *Cross section measurement of t-channel single top quark production in pp collisions at* $\sqrt{s} = 13$ *TeV*, *Phys. Lett. B* **772** (2017) 752 [arXiv:1610.00678] [INSPIRE].

[11] ATLAS collaboration, *Measurement of the inclusive cross-sections of single top-quark and top-antiquark t-channel production in pp collisions at $\sqrt{s} = 13$ TeV with the ATLAS detector*, *JHEP* **04** (2017) 086 [arXiv:1609.03920] [INSPIRE].

[12] CMS collaboration, *Observation of tW production in the single-lepton channel in pp collisions at $\sqrt{s} = 13$ TeV*, *JHEP* **11** (2021) 111 [arXiv:2109.01706] [INSPIRE].

[13] ATLAS collaboration, *Measurement of the cross-section for producing a W boson in association with a single top quark in pp collisions at $\sqrt{s} = 13$ TeV with ATLAS*, *JHEP* **01** (2018) 063 [arXiv:1612.07231] [INSPIRE].

[14] CMS collaboration, *Search for s channel single top quark production in pp collisions at $\sqrt{s} = 7$ and 8 TeV*, *JHEP* **09** (2016) 027 [arXiv:1603.02555] [INSPIRE].

[15] ATLAS collaboration, *Evidence for single top-quark production in the s-channel in proton-proton collisions at $\sqrt{s} = 8$ TeV with the ATLAS detector using the Matrix Element Method*, *Phys. Lett. B* **756** (2016) 228 [arXiv:1511.05980] [INSPIRE].

[16] K. Kondo, *Dynamical Likelihood Method for Reconstruction of Events With Missing Momentum. 1: Method and Toy Models*, *J. Phys. Soc. Jap.* **57** (1988) 4126 [INSPIRE].

[17] K. Kondo, *Dynamical likelihood method for reconstruction of events with missing momentum. 2: Mass spectra for $2 \to 2$ processes*, *J. Phys. Soc. Jap.* **60** (1991) 836 [INSPIRE].

[18] ATLAS collaboration, *Search for s-channel single top-quark production in proton–proton collisions at $\sqrt{s} = 8$ TeV with the ATLAS detector*, *Phys. Lett. B* **740** (2015) 118 [arXiv:1410.0647] [INSPIRE].

[19] ATLAS collaboration, *The ATLAS Experiment at the CERN Large Hadron Collider*, 2008 *JINST* **3** S08003 [INSPIRE].

[20] ATLAS collaboration, *The ATLAS collaboration software and firmware*, ATL-SOFT-PUB-2021-001, CERN, Geneva (2021).

[21] ATLAS collaboration, *ATLAS data quality operations and performance for 2015–2018 data-taking*, 2020 *JINST* **15** P04003 [arXiv:1911.04632] [INSPIRE].

[22] ATLAS collaboration, *The ATLAS simulation infrastructure*, *Eur. Phys. J. C* **70** (2010) 823 [arXiv:1005.4568] [INSPIRE].

[23] GEANT4 collaboration, *GEANT4 — a simulation toolkit*, *Nucl. Instrum. Meth. A* **506** (2003) 250 [INSPIRE].

[24] T. Sjöstrand et al., *An introduction to PYTHIA 8.2*, *Comput. Phys. Commun.* **191** (2015) 159 [arXiv:1410.3012] [INSPIRE].

[25] ATLAS collaboration, *The Pythia 8 A3 tune description of ATLAS minimum bias and inelastic measurements incorporating the Donnachie-Landshoff diffractive model*, ATL-PHYS-PUB-2016-017, CERN, Geneva (2016).

[26] P. Nason, *A New method for combining NLO QCD with shower Monte Carlo algorithms*, *JHEP* **11** (2004) 040 [hep-ph/0409146] [INSPIRE].

[27] S. Frixione, P. Nason and C. Oleari, *Matching NLO QCD computations with Parton Shower simulations: the POWHEG method*, *JHEP* **11** (2007) 070 [arXiv:0709.2092] [INSPIRE].

[28] S. Alioli, P. Nason, C. Oleari and E. Re, *A general framework for implementing NLO*

calculations in shower Monte Carlo programs: the POWHEG BOX, JHEP **06** (2010) 043 [arXiv:1002.2581] [INSPIRE].

[29] S. Alioli, P. Nason, C. Oleari and E. Re, *NLO single-top production matched with shower in POWHEG: s- and t-channel contributions*, JHEP **09** (2009) 111 [*Erratum ibid.* **02** (2010) 011] [arXiv:0907.4076] [INSPIRE].

[30] R. Frederix, E. Re and P. Torrielli, *Single-top t-channel hadroproduction in the four-flavour scheme with POWHEG and aMC@NLO*, JHEP **09** (2012) 130 [arXiv:1207.5391] [INSPIRE].

[31] E. Re, *Single-top Wt-channel production matched with parton showers using the POWHEG method*, Eur. Phys. J. C **71** (2011) 1547 [arXiv:1009.2450] [INSPIRE].

[32] S. Frixione, P. Nason and G. Ridolfi, *A positive-weight next-to-leading-order Monte Carlo for heavy flavour hadroproduction*, JHEP **09** (2007) 126 [arXiv:0707.3088] [INSPIRE].

[33] R.D. Ball, *Parton distributions for the LHC Run II*, JHEP **04** (2015) 040 [arXiv:1410.8849] [INSPIRE].

[34] ATLAS collaboration, *ATLAS Pythia 8 tunes to* 7 *TeV data*, ATL-PHYS-PUB-2014-021 (2014).

[35] R.D. Ball et al., *Parton distributions with LHC data*, Nucl. Phys. B **867** (2013) 244 [arXiv:1207.1303] [INSPIRE].

[36] D.J. Lange, *The EvtGen particle decay simulation package*, Nucl. Instrum. Meth. A **462** (2001) 152 [INSPIRE].

[37] S. Frixione et al., *Single-top hadroproduction in association with a W boson*, JHEP **07** (2008) 029 [arXiv:0805.3067] [INSPIRE].

[38] M. Bähr et al., *Herwig++ physics and manual*, Eur. Phys. J. C **58** (2008) 639 [arXiv:0803.0883] [INSPIRE].

[39] J. Bellm et al., *Herwig 7.0/Herwig++ 3.0 release note*, Eur. Phys. J. C **76** (2016) 196 [arXiv:1512.01178] [INSPIRE].

[40] L.A. Harland-Lang, A.D. Martin, P. Motylinski and R.S. Thorne, *Parton distributions in the LHC era: MMHT 2014 PDFs*, Eur. Phys. J. C **75** (2015) 204 [arXiv:1412.3989] [INSPIRE].

[41] SHERPA collaboration, *Event generation with Sherpa 2.2*, SciPost Phys. **7** (2019) 034 [arXiv:1905.09127] [INSPIRE].

[42] T. Gleisberg and S. Höche, *Comix, a new matrix element generator*, JHEP **12** (2008) 039 [arXiv:0808.3674] [INSPIRE].

[43] F. Buccioni et al., *OpenLoops 2*, Eur. Phys. J. C **79** (2019) 866 [arXiv:1907.13071] [INSPIRE].

[44] F. Cascioli, P. Maierhöfer and S. Pozzorini, *Scattering Amplitudes with Open Loops*, Phys. Rev. Lett. **108** (2012) 111601 [arXiv:1111.5206] [INSPIRE].

[45] A. Denner, S. Dittmaier and L. Hofer, *Collier: a Fortran-based Complex One-Loop LIbrary in Extended Regularizations*, Comput. Phys. Commun. **212** (2017) 220 [arXiv:1604.06792] [INSPIRE].

[46] S. Schumann and F. Krauss, *A Parton shower algorithm based on Catani-Seymour dipole factorisation*, JHEP **03** (2008) 038 [arXiv:0709.1027] [INSPIRE].

[47] S. Höche, F. Krauss, M. Schönherr and F. Siegert, *A critical appraisal of NLO+PS matching methods*, *JHEP* **09** (2012) 049 [arXiv:1111.1220] [INSPIRE].

[48] S. Höche, F. Krauss, M. Schönherr and F. Siegert, *QCD matrix elements + parton showers: The NLO case*, *JHEP* **04** (2013) 027 [arXiv:1207.5030] [INSPIRE].

[49] S. Catani, F. Krauss, R. Kuhn and B.R. Webber, *QCD matrix elements + parton showers*, *JHEP* **11** (2001) 063 [hep-ph/0109231] [INSPIRE].

[50] S. Höche, F. Krauss, S. Schumann and F. Siegert, *QCD matrix elements and truncated showers*, *JHEP* **05** (2009) 053 [arXiv:0903.1219] [INSPIRE].

[51] M. Aliev et al., *HATHOR: HAdronic Top and Heavy quarks crOss section calculatoR*, *Comput. Phys. Commun.* **182** (2011) 1034 [arXiv:1007.1327] [INSPIRE].

[52] P. Kant et al., *HatHor for single top-quark production: Updated predictions and uncertainty estimates for single top-quark production in hadronic collisions*, *Comput. Phys. Commun.* **191** (2015) 74 [arXiv:1406.4403] [INSPIRE].

[53] J. Butterworth et al., *PDF4LHC recommendations for LHC Run II*, *J. Phys. G* **43** (2016) 023001 [arXiv:1510.03865] [INSPIRE].

[54] A.D. Martin, W.J. Stirling, R.S. Thorne and G. Watt, *Parton distributions for the LHC*, *Eur. Phys. J. C* **63** (2009) 189 [arXiv:0901.0002] [INSPIRE].

[55] A.D. Martin, W.J. Stirling, R.S. Thorne and G. Watt, *Uncertainties on alpha(S) in global PDF analyses and implications for predicted hadronic cross sections*, *Eur. Phys. J. C* **64** (2009) 653 [arXiv:0905.3531] [INSPIRE].

[56] H.-L. Lai et al., *New parton distributions for collider physics*, *Phys. Rev. D* **82** (2010) 074024 [arXiv:1007.2241] [INSPIRE].

[57] M. Beneke, P. Falgari, S. Klein and C. Schwinn, *Hadronic top-quark pair production with NNLL threshold resummation*, *Nucl. Phys. B* **855** (2012) 695 [arXiv:1109.1536] [INSPIRE].

[58] M. Cacciari et al., *Top-pair production at hadron colliders with next-to-next-to-leading logarithmic soft-gluon resummation*, *Phys. Lett. B* **710** (2012) 612 [arXiv:1111.5869] [INSPIRE].

[59] P. Bärnreuther, M. Czakon and A. Mitov, *Percent Level Precision Physics at the Tevatron: First Genuine NNLO QCD Corrections to $q\bar{q} \to t\bar{t} + X$*, *Phys. Rev. Lett.* **109** (2012) 132001 [arXiv:1204.5201] [INSPIRE].

[60] M. Czakon and A. Mitov, *NNLO corrections to top-pair production at hadron colliders: the all-fermionic scattering channels*, *JHEP* **12** (2012) 054 [arXiv:1207.0236] [INSPIRE].

[61] M. Czakon and A. Mitov, *NNLO corrections to top pair production at hadron colliders: the quark-gluon reaction*, *JHEP* **01** (2013) 080 [arXiv:1210.6832] [INSPIRE].

[62] M. Czakon, P. Fiedler and A. Mitov, *Total Top-Quark Pair-Production Cross section at Hadron Colliders Through $O(\alpha_S^4)$*, *Phys. Rev. Lett.* **110** (2013) 252004 [arXiv:1303.6254] [INSPIRE].

[63] M. Czakon and A. Mitov, *Top++: a program for the calculation of the top-pair cross-section at hadron colliders*, *Comput. Phys. Commun.* **185** (2014) 2930 [arXiv:1112.5675] [INSPIRE].

[64] J. Gao et al., *CT10 next-to-next-to-leading order global analysis of QCD*, *Phys. Rev. D* **89** (2014) 033009 [arXiv:1302.6246] [INSPIRE].

[65] N. Kidonakis, *Two-loop soft anomalous dimensions for single top quark associated production with a W^- or H^-*, *Phys. Rev. D* **82** (2010) 054018 [arXiv:1005.4451] [INSPIRE].

[66] N. Kidonakis, *Top Quark Production*, [DOI:10.3204/DESY-PROC-2013-03/Kidonakis] [arXiv:1311.0283] [INSPIRE].

[67] C. Anastasiou, L.J. Dixon, K. Melnikov and F. Petriello, *High precision QCD at hadron colliders: Electroweak gauge boson rapidity distributions at NNLO*, *Phys. Rev. D* **69** (2004) 094008 [hep-ph/0312266] [INSPIRE].

[68] K. Melnikov and F. Petriello, *Electroweak gauge boson production at hadron colliders through $O(\alpha_s^2)$*, *Phys. Rev. D* **74** (2006) 114017 [hep-ph/0609070] [INSPIRE].

[69] ATLAS collaboration, *Reconstruction of primary vertices at the ATLAS experiment in Run 1 proton–proton collisions at the LHC*, *Eur. Phys. J. C* **77** (2017) 332 [arXiv:1611.10235] [INSPIRE].

[70] ATLAS collaboration, *Performance of the ATLAS muon triggers in Run 2*, 2020 *JINST* **15** P09015 [arXiv:2004.13447] [INSPIRE].

[71] ATLAS collaboration, *Performance of electron and photon triggers in ATLAS during LHC Run 2*, *Eur. Phys. J. C* **80** (2020) 47 [arXiv:1909.00761] [INSPIRE].

[72] ATLAS collaboration, *Electron and photon performance measurements with the ATLAS detector using the 2015–2017 LHC proton-proton collision data*, 2019 *JINST* **14** P12006 [arXiv:1908.00005] [INSPIRE].

[73] ATLAS collaboration, *Muon reconstruction and identification efficiency in ATLAS using the full Run 2 pp collision data set at $\sqrt{s} = 13$ TeV*, *Eur. Phys. J. C* **81** (2021) 578 [arXiv:2012.00578] [INSPIRE].

[74] ATLAS collaboration, *Topological cell clustering in the ATLAS calorimeters and its performance in LHC Run 1*, *Eur. Phys. J. C* **77** (2017) 490 [arXiv:1603.02934] [INSPIRE].

[75] ATLAS collaboration, *Jet energy scale and resolution measured in proton–proton collisions at $\sqrt{s} = 13$ TeV with the ATLAS detector*, *Eur. Phys. J. C* **81** (2021) 689 [arXiv:2007.02645] [INSPIRE].

[76] M. Cacciari, G.P. Salam and G. Soyez, *The anti-k_t jet clustering algorithm*, *JHEP* **04** (2008) 063 [arXiv:0802.1189] [INSPIRE].

[77] M. Cacciari, G.P. Salam and G. Soyez, *FastJet user manual*, *Eur. Phys. J. C* **72** (2012) 1896 [arXiv:1111.6097] [INSPIRE].

[78] ATLAS collaboration, *Performance of pile-up mitigation techniques for jets in pp collisions at $\sqrt{s} = 8$ TeV using the ATLAS detector*, *Eur. Phys. J. C* **76** (2016) 581 [arXiv:1510.03823] [INSPIRE].

[79] ATLAS collaboration, *ATLAS b-jet identification performance and efficiency measurement with $t\bar{t}$ events in pp collisions at $\sqrt{s} = 13$ TeV*, *Eur. Phys. J. C* **79** (2019) 970 [arXiv:1907.05120] [INSPIRE].

[80] ATLAS collaboration, *Measurement of b-tagging Efficiency of c-jets in $t\bar{t}$ Events Using a Likelihood Approach with the ATLAS Detector*, ATLAS-CONF-2018-001, CERN, Geneva (2018).

[81] ATLAS collaboration, *Calibration of light-flavour b-jet mistagging rates using ATLAS proton-proton collision data at $\sqrt{s} = 13$ TeV*, ATLAS-CONF-2018-006, CERN, Geneva (2018).

[82] ATLAS collaboration, *Performance of missing transverse momentum reconstruction with the ATLAS detector using proton-proton collisions at $\sqrt{s} = 13$ TeV*, *Eur. Phys. J. C* **78** (2018) 903 [arXiv:1802.08168] [INSPIRE].

[83] ATLAS collaboration, *Muon reconstruction performance of the ATLAS detector in proton–proton collision data at $\sqrt{s} = 13$ TeV*, *Eur. Phys. J. C* **76** (2016) 292 [arXiv:1603.05598] [INSPIRE].

[84] ATLAS collaboration, *Estimation of non-prompt and fake lepton backgrounds in final states with top quarks produced in proton-proton collisions at $\sqrt{s} = 8$ TeV with the ATLAS detector*, ATLAS-CONF-2014-058, CERN, Geneva (2014).

[85] ATLAS collaboration, *Fiducial, total and differential cross-section measurements of t-channel single top-quark production in pp collisions at 8 TeV using data collected by the ATLAS detector*, *Eur. Phys. J. C* **77** (2017) 531 [arXiv:1702.02859] [INSPIRE].

[86] ATLAS collaboration, *Measurement of the $t\bar{t}$ production cross-section in the lepton+jets channel at $\sqrt{s} = 13$ TeV with the ATLAS experiment*, *Phys. Lett. B* **810** (2020) 135797 [arXiv:2006.13076] [INSPIRE].

[87] CDF collaboration, *Measurement of the single top quark production cross section at CDF*, *Phys. Rev. Lett.* **101** (2008) 252001 [arXiv:0809.2581] [INSPIRE].

[88] D0 collaboration, *Evidence for production of single top quarks and first direct measurement of $|V_{tb}|$*, *Phys. Rev. Lett.* **98** (2007) 181802 [hep-ex/0612052] [INSPIRE].

[89] D0 collaboration, *Evidence for production of single top quarks*, *Phys. Rev. D* **78** (2008) 012005 [arXiv:0803.0739] [INSPIRE].

[90] G.P. Lepage, *A new algorithm for adaptive multidimensional integration*, *J. Comput. Phys.* **27** (1978) 192 [INSPIRE].

[91] T. Hahn, *The CUBA library*, *Nucl. Instrum. Meth. A* **559** (2006) 273 [hep-ph/0509016] [INSPIRE].

[92] J.R. Andersen et al., *Les Houches 2013: Physics at TeV Colliders: Standard Model Working Group Report*, arXiv:1405.1067 [INSPIRE].

[93] J.M. Campbell and R.K. Ellis, *MCFM for the Tevatron and the LHC*, *Nucl. Phys. B Proc. Suppl.* **205-206** (2010) 10 [arXiv:1007.3492] [INSPIRE].

[94] ATLAS collaboration, *Measurement of the charge asymmetry in top quark pair production in pp collisions at $\sqrt{s} = 7$ TeV using the ATLAS detector*, *Eur. Phys. J. C* **72** (2012) 2039 [arXiv:1203.4211] [INSPIRE].

[95] J. Erdmann et al., *A likelihood-based reconstruction algorithm for top-quark pairs and the KLFitter framework*, *Nucl. Instrum. Meth. A* **748** (2014) 18 [arXiv:1312.5595] [INSPIRE].

[96] ATLAS collaboration, *Luminosity determination in pp collisions at $\sqrt{s} = 13$ TeV using the ATLAS detector at the LHC*, ATLAS-CONF-2019-021, CERN, Geneva (2019).

[97] G. Avoni et al., *The new LUCID-2 detector for luminosity measurement and monitoring in ATLAS*, 2018 *JINST* **13** P07017 [INSPIRE].

JHEP06(2023)191

[98] ATLAS collaboration, *Measurement of the Inelastic Proton-Proton Cross section at $\sqrt{s} = 13$ TeV with the ATLAS Detector at the LHC*, Phys. Rev. Lett. **117** (2016) 182002 [arXiv:1606.02625] [INSPIRE].

[99] S.D. Ellis, R. Kleiss and W.J. Stirling, *W's, Z's and Jets*, Phys. Lett. B **154** (1985) 435 [INSPIRE].

[100] F.A. Berends, H. Kuijf, B. Tausk and W.T. Giele, *On the production of a W and jets at hadron colliders*, Nucl. Phys. B **357** (1991) 32 [INSPIRE].

[101] ATLAS collaboration, *Search for the $b\bar{b}$ decay of the Standard Model Higgs boson in associated $(W/Z)H$ production with the ATLAS detector*, JHEP **01** (2015) 069 [arXiv:1409.6212] [INSPIRE].

[102] G. Cowan, K. Cranmer, E. Gross and O. Vitells, *Asymptotic formulae for likelihood-based tests of new physics*, Eur. Phys. J. C **71** (2011) 1554 [*Erratum ibid.* **73** (2013) 2501] [arXiv:1007.1727] [INSPIRE].

[103] W. Verkerke and D. Kirkby, *The RooFit toolkit for data modeling*, physics/0306116.

[104] L. Moneta et al., *The RooStats project*, PoS **ACAT2010** (2011) 057 [arXiv:1009.1003] [INSPIRE].

[105] K. Cranmer et al., *HistFactory: A tool for creating statistical models for use with RooFit and RooStats*, CERN-OPEN-2012-016, New York University, New York (2012).

[106] R.D. Cousins, *Generalization of chisquare goodness-of-fit test for binned data using saturated models, with application to histograms*, http://www.physics.ucla.edu/~cousins/stats/cousins_saturated.pdf.

[107] ATLAS collaboration, *ATLAS Computing Acknowledgements*, ATL-SOFT-PUB-2021-003 (2021).

The ATLAS collaboration

G. Aad[101], B. Abbott[119], D.C. Abbott[102], K. Abeling[55], S.H. Abidi[29], A. Aboulhorma[35e], H. Abramowicz[150], H. Abreu[149], Y. Abulaiti[116], A.C. Abusleme Hoffman[136a], B.S. Acharya[68a,68b,o], B. Achkar[55], C. Adam Bourdarios[4], L. Adamczyk[84a], L. Adamek[154], S.V. Addepalli[26], J. Adelman[114], A. Adiguzel[21c], S. Adorni[56], T. Adye[133], A.A. Affolder[135], Y. Afik[36], M.N. Agaras[13], J. Agarwala[72a,72b], A. Aggarwal[99], C. Agheorghiesei[27c], J.A. Aguilar-Saavedra[129f], A. Ahmad[36], F. Ahmadov[38,w], W.S. Ahmed[103], S. Ahuja[94], X. Ai[48], G. Aielli[75a,75b], I. Aizenberg[167], M. Akbiyik[99], T.P.A. Åkesson[97], A.V. Akimov[37], K. Al Khoury[41], G.L. Alberghi[23b], J. Albert[163], P. Albicocco[53], M.J. Alconada Verzini[89], S. Alderweireldt[52], M. Aleksa[36], I.N. Aleksandrov[38], C. Alexa[27b], T. Alexopoulos[10], A. Alfonsi[113], F. Alfonsi[23b], M. Alhroob[119], B. Ali[131], S. Ali[147], M. Aliev[37], G. Alimonti[70a], W. Alkakhi[55], C. Allaire[36], B.M.M. Allbrooke[145], P.P. Allport[20], A. Aloisio[71a,71b], F. Alonso[89], C. Alpigiani[137], E. Alunno Camelia[75a,75b], M. Alvarez Estevez[98], M.G. Alviggi[71a,71b], Y. Amaral Coutinho[81b], A. Ambler[103], C. Amelung[36], C.G. Ames[108], D. Amidei[105], S.P. Amor Dos Santos[129a], S. Amoroso[48], K.R. Amos[161], C.S. Amrouche[56], V. Ananiev[124], C. Anastopoulos[138], T. Andeen[11], J.K. Anders[19], S.Y. Andrean[47a,47b], A. Andreazza[70a,70b], S. Angelidakis[9], A. Angerami[41,y], A.V. Anisenkov[37], A. Annovi[73a], C. Antel[56], M.T. Anthony[138], E. Antipov[120], M. Antonelli[53], D.J.A. Antrim[17a], F. Anulli[74a], M. Aoki[82], T. Aoki[152], J.A. Aparisi Pozo[161], M.A. Aparo[145], L. Aperio Bella[48], C. Appelt[18], N. Aranzabal[36], V. Araujo Ferraz[81a], C. Arcangeletti[53], A.T.H. Arce[51], E. Arena[91], J-F. Arguin[107], S. Argyropoulos[54], J.-H. Arling[48], A.J. Armbruster[36], O. Arnaez[154], H. Arnold[113], Z.P. Arrubarrena Tame[108], G. Artoni[74a,74b], H. Asada[110], K. Asai[117], S. Asai[152], N.A. Asbah[61], J. Assahsah[35d], K. Assamagan[29], R. Astalos[28a], R.J. Atkin[33a], M. Atkinson[160], N.B. Atlay[18], H. Atmani[62b], P.A. Atmasiddha[105], K. Augsten[131], S. Auricchio[71a,71b], A.D. Auriol[20], V.A. Austrup[169], G. Avner[149], G. Avolio[36], K. Axiotis[56], M.K. Ayoub[14c], G. Azuelos[107,aa], D. Babal[28a], H. Bachacou[134], K. Bachas[151,q], A. Bachiu[34], F. Backman[47a,47b], A. Badea[61], P. Bagnaia[74a,74b], M. Bahmani[18], A.J. Bailey[161], V.R. Bailey[160], J.T. Baines[133], C. Bakalis[10], O.K. Baker[170], P.J. Bakker[113], E. Bakos[15], D. Bakshi Gupta[8], S. Balaji[146], R. Balasubramanian[113], E.M. Baldin[37], P. Balek[132], E. Ballabene[70a,70b], F. Balli[134], L.M. Baltes[63a], W.K. Balunas[32], J. Balz[99], E. Banas[85], M. Bandieramonte[128], A. Bandyopadhyay[24], S. Bansal[24], L. Barak[150], E.L. Barberio[104], D. Barberis[57b,57a], M. Barbero[101], G. Barbour[95], K.N. Barends[33a], T. Barillari[109], M-S. Barisits[36], T. Barklow[142], R.M. Barnett[17a], P. Baron[121], D.A. Baron Moreno[100], A. Baroncelli[62a], G. Barone[29], A.J. Barr[125], L. Barranco Navarro[47a,47b], F. Barreiro[98], J. Barreiro Guimarães da Costa[14a], U. Barron[150], M.G. Barros Teixeira[129a], S. Barsov[37], F. Bartels[63a], R. Bartoldus[142], A.E. Barton[90], P. Bartos[28a], A. Basalaev[48], A. Basan[99], M. Baselga[49], I. Bashta[76a,76b], A. Bassalat[66,ag], M.J. Basso[154], C.R. Basson[100], R.L. Bates[59], S. Batlamous[35e], J.R. Batley[32], B. Batool[140], M. Battaglia[135], D. Battulga[18], M. Bauce[74a,74b], P. Bauer[24], A. Bayirli[21a],

JHEP06(2023)191

J.B. Beacham[51], T. Beau[126], P.H. Beauchemin[157], F. Becherer[54], P. Bechtle[24], H.P. Beck[19,p], K. Becker[165], C. Becot[48], A.J. Beddall[21d], V.A. Bednyakov[38], C.P. Bee[144], L.J. Beemster[15], T.A. Beermann[36], M. Begalli[81d,81d], M. Begel[29], A. Behera[144], J.K. Behr[48], C. Beirao Da Cruz E Silva[36], J.F. Beirer[55,36], F. Beisiegel[24], M. Belfkir[115b], G. Bella[150], L. Bellagamba[23b], A. Bellerive[34], P. Bellos[20], K. Beloborodov[37], K. Belotskiy[37], N.L. Belyaev[37], D. Benchekroun[35a], F. Bendebba[35a], Y. Benhammou[150], D.P. Benjamin[29], M. Benoit[29], J.R. Bensinger[26], S. Bentvelsen[113], L. Beresford[36], M. Beretta[53], D. Berge[18], E. Bergeaas Kuutmann[159], N. Berger[4], B. Bergmann[131], J. Beringer[17a], S. Berlendis[7], G. Bernardi[5], C. Bernius[142], F.U. Bernlochner[24], T. Berry[94], P. Berta[132], A. Berthold[50], I.A. Bertram[90], S. Bethke[109], A. Betti[74a,74b], A.J. Bevan[93], M. Bhamjee[33c], S. Bhatta[144], D.S. Bhattacharya[164], P. Bhattarai[26], V.S. Bhopatkar[120], R. Bi[29,ad], R.M. Bianchi[128], O. Biebel[108], R. Bielski[122], M. Biglietti[76a], T.R.V. Billoud[131], M. Bindi[55], A. Bingul[21b], C. Bini[74a,74b], S. Biondi[23b,23a], A. Biondini[91], C.J. Birch-sykes[100], G.A. Bird[20,133], M. Birman[167], T. Bisanz[36], E. Bisceglie[43b,43a], D. Biswas[168,k], A. Bitadze[100], K. Bjørke[124], I. Bloch[48], C. Blocker[26], A. Blue[59], U. Blumenschein[93], J. Blumenthal[99], G.J. Bobbink[113], V.S. Bobrovnikov[37], M. Boehler[54], D. Bogavac[36], A.G. Bogdanchikov[37], C. Bohm[47a], V. Boisvert[94], P. Bokan[48], T. Bold[84a], M. Bomben[5], M. Bona[93], M. Boonekamp[134], C.D. Booth[94], A.G. Borbély[59], H.M. Borecka-Bielska[107], L.S. Borgna[95], G. Borissov[90], D. Bortoletto[125], D. Boscherini[23b], M. Bosman[13], J.D. Bossio Sola[36], K. Bouaouda[35a], J. Boudreau[128], E.V. Bouhova-Thacker[90], D. Boumediene[40], R. Bouquet[5], A. Boveia[118], J. Boyd[36], D. Boye[29], I.R. Boyko[38], J. Bracinik[20], N. Brahimi[62d], G. Brandt[169], O. Brandt[32], F. Braren[48], B. Brau[102], J.E. Brau[122], K. Brendlinger[48], R. Brener[167], L. Brenner[36], R. Brenner[159], S. Bressler[167], B. Brickwedde[99], D. Britton[59], D. Britzger[109], I. Brock[24], G. Brooijmans[41], W.K. Brooks[136f], E. Brost[29], T.L. Bruckler[125], P.A. Bruckman de Renstrom[85], B. Brüers[48], D. Bruncko[28b,*], A. Bruni[23b], G. Bruni[23b], M. Bruschi[23b], N. Bruscino[74a,74b], L. Bryngemark[142], T. Buanes[16], Q. Buat[137], P. Buchholz[140], A.G. Buckley[59], I.A. Budagov[38,*], M.K. Bugge[124], O. Bulekov[37], B.A. Bullard[61], S. Burdin[91], C.D. Burgard[48], A.M. Burger[40], B. Burghgrave[8], J.T.P. Burr[32], C.D. Burton[11], J.C. Burzynski[141], E.L. Busch[41], V. Büscher[99], P.J. Bussey[59], J.M. Butler[25], C.M. Buttar[59], J.M. Butterworth[95], W. Buttinger[133], C.J. Buxo Vazquez[106], A.R. Buzykaev[37], G. Cabras[23b], S. Cabrera Urbán[161], D. Caforio[58], H. Cai[128], Y. Cai[14a,14d], V.M.M. Cairo[36], O. Cakir[3a], N. Calace[36], P. Calafiura[17a], G. Calderini[126], P. Calfayan[67], G. Callea[59], L.P. Caloba[81b], D. Calvet[40], S. Calvet[40], T.P. Calvet[101], M. Calvetti[73a,73b], R. Camacho Toro[126], S. Camarda[36], D. Camarero Munoz[26], P. Camarri[75a,75b], M.T. Camerlingo[76a,76b], D. Cameron[124], C. Camincher[163], M. Campanelli[95], A. Camplani[42], V. Canale[71a,71b], A. Canesse[103], M. Cano Bret[79], J. Cantero[161], Y. Cao[160], F. Capocasa[26], M. Capua[43b,43a], A. Carbone[70a,70b], R. Cardarelli[75a], J.C.J. Cardenas[8], F. Cardillo[161], T. Carli[36], G. Carlino[71a], J.I. Carlotto[13], B.T. Carlson[128,r], E.M. Carlson[163,155a], L. Carminati[70a,70b], M. Carnesale[74a,74b], S. Caron[112], E. Carquin[136f], S. Carrá[70a,70b], G. Carratta[23b,23a], F. Carrio Argos[33g], J.W.S. Carter[154], T.M. Carter[52], M.P. Casado[13,h], A.F. Casha[154], E.G. Castiglia[170], F.L. Castillo[63a], L. Castillo Garcia[13], V. Castillo Gimenez[161], N.F. Castro[129a,129e], A. Catinaccio[36], J.R. Catmore[124], V. Cavaliere[29], N. Cavalli[23b,23a], V. Cavasinni[73a,73b], E. Celebi[21a], F. Celli[125], M.S. Centonze[69a,69b], K. Cerny[121], A.S. Cerqueira[81a], A. Cerri[145], L. Cerrito[75a,75b], F. Cerutti[17a], A. Cervelli[23b], S.A. Cetin[21d], Z. Chadi[35a], D. Chakraborty[114], M. Chala[129f], J. Chan[168], W.Y. Chan[152], J.D. Chapman[32], B. Chargeishvili[148b], D.G. Charlton[20], T.P. Charman[93], M. Chatterjee[19], S. Chekanov[6], S.V. Chekulaev[155a], G.A. Chelkov[38,a], A. Chen[105], B. Chen[150], B. Chen[163], C. Chen[62a], H. Chen[14c], H. Chen[29], J. Chen[62c], J. Chen[26], S. Chen[152], S.J. Chen[14c], X. Chen[62c], X. Chen[14b,z], Y. Chen[62a], C.L. Cheng[168], H.C. Cheng[64a], A. Cheplakov[38], E. Cheremushkina[48], E. Cherepanova[113], R. Cherkaoui El Moursli[35e], E. Cheu[7], K. Cheung[65], L. Chevalier[134], V. Chiarella[53], G. Chiarelli[73a], N. Chiedde[101], G. Chiodini[69a], A.S. Chisholm[20], A. Chitan[27b], M. Chitishvili[161], Y.H. Chiu[163], M.V. Chizhov[38], K. Choi[11], A.R. Chomont[74a,74b], Y. Chou[102], E.Y.S. Chow[113], T. Chowdhury[33g], L.D. Christopher[33g], K.L. Chu[64a], M.C. Chu[64a], X. Chu[14a,14d], J. Chudoba[130], J.J. Chwastowski[85], D. Cieri[109], K.M. Ciesla[84a], V. Cindro[92], A. Ciocio[17a], F. Cirotto[71a,71b], Z.H. Citron[167,l], M. Citterio[70a], D.A. Ciubotaru[27b], B.M. Ciungu[154], A. Clark[56], P.J. Clark[52], J.M. Clavijo Columbie[48], S.E. Clawson[100], C. Clement[47a,47b], J. Clercx[48], L. Clissa[23b,23a], Y. Coadou[101], M. Cobal[68a,68c], A. Coccaro[57b], R.F. Coelho Barrue[129a], R. Coelho Lopes De Sa[102], S. Coelli[70a], H. Cohen[150], A.E.C. Coimbra[70a,70b], B. Cole[41], J. Collot[60], P. Conde Muiño[129a,129g], M.P. Connell[33c], S.H. Connell[33c], I.A. Connelly[59], E.I. Conroy[125], F. Conventi[71a,ab], H.G. Cooke[20], A.M. Cooper-Sarkar[125], F. Cormier[162], L.D. Corpe[36], M. Corradi[74a,74b], E.E. Corrigan[97], F. Corriveau[103,v], A. Cortes-Gonzalez[18], M.J. Costa[161], F. Costanza[4], D. Costanzo[138], B.M. Cote[118], G. Cowan[94], J.W. Cowley[32], K. Cranmer[116], S. Crépé-Renaudin[60], F. Crescioli[126], M. Cristinziani[140], M. Cristoforetti[77a,77b,c], V. Croft[157], G. Crosetti[43b,43a], A. Cueto[36], T. Cuhadar Donszelmann[158], H. Cui[14a,14d], Z. Cui[7], A.R. Cukierman[142], W.R. Cunningham[59], F. Curcio[43b,43a], P. Czodrowski[36], M.M. Czurylo[63b], M.J. Da Cunha Sargedas De Sousa[62a], J.V. Da Fonseca Pinto[81b], C. Da Via[100], W. Dabrowski[84a], T. Dado[49], S. Dahbi[33g], T. Dai[105], C. Dallapiccola[102], M. Dam[42], G. D'amen[29], V. D'Amico[108], J. Damp[99], J.R. Dandoy[127], M.F. Daneri[30], M. Danninger[141], V. Dao[36], G. Darbo[57b], S. Darmora[6], S.J. Das[29], S. D'Auria[70a,70b], C. David[155b], T. Davidek[132], D.R. Davis[51], B. Davis-Purcell[34], I. Dawson[93], K. De[8], R. De Asmundis[71a], M. De Beurs[113], N. De Biase[48], S. De Castro[23b,23a], N. De Groot[112], P. de Jong[113], H. De la Torre[106], A. De Maria[14c], A. De Salvo[74a], U. De Sanctis[75a,75b], A. De Santo[145], J.B. De Vivie De Regie[60], D.V. Dedovich[38], J. Degens[113], A.M. Deiana[44], F. Del Corso[23b,23a], J. Del Peso[98], F. Del Rio[63a], F. Deliot[134], C.M. Delitzsch[49], M. Della Pietra[71a,71b], D. Della Volpe[56], A. Dell'Acqua[36], L. Dell'Asta[70a,70b], M. Delmastro[4], P.A. Delsart[60], S. Demers[170], M. Demichev[38], S.P. Denisov[37], L. D'Eramo[114], D. Derendarz[85], F. Derue[126], P. Dervan[91], K. Desch[24], K. Dette[154], C. Deutsch[24], P.O. Deviveiros[36], F.A. Di Bello[74a,74b], A. Di Ciaccio[75a,75b], L. Di Ciaccio[4], A. Di Domenico[74a,74b], C. Di Donato[71a,71b], A. Di Girolamo[36],

JHEP06(2023)191

G. Di Gregorio[73a,73b], A. Di Luca[77a,77b], B. Di Micco[76a,76b], R. Di Nardo[76a,76b], C. Diaconu[101], F.A. Dias[113], T. Dias Do Vale[141], M.A. Diaz[136a,136b], F.G. Diaz Capriles[24], M. Didenko[161], E.B. Diehl[105], L. Diehl[54], S. Díez Cornell[48], C. Diez Pardos[140], C. Dimitriadi[24,159], A. Dimitrievska[17a], W. Ding[14b], J. Dingfelder[24], I-M. Dinu[27b], S.J. Dittmeier[63b], F. Dittus[36], F. Djama[101], T. Djobava[148b], J.I. Djuvsland[16], C. Doglioni[100,97], J. Dolejsi[132], Z. Dolezal[132], M. Donadelli[81c], B. Dong[62c], J. Donini[40], A. D'Onofrio[14c], M. D'Onofrio[91], J. Dopke[133], A. Doria[71a], M.T. Dova[89], A.T. Doyle[59], M.A. Draguet[125], E. Drechsler[141], E. Dreyer[167], I. Drivas-koulouris[10], A.S. Drobac[157], M. Drozdova[56], D. Du[62a], T.A. du Pree[113], F. Dubinin[37], M. Dubovsky[28a], E. Duchovni[167], G. Duckeck[108], O.A. Ducu[27b], D. Duda[109], A. Dudarev[36], M. D'uffizi[100], L. Duflot[66], M. Dührssen[36], C. Dülsen[169], A.E. Dumitriu[27b], M. Dunford[63a], S. Dungs[49], K. Dunne[47a,47b], A. Duperrin[101], H. Duran Yildiz[3a], M. Düren[58], A. Durglishvili[148b], B.L. Dwyer[114], G.I. Dyckes[17a], M. Dyndal[84a], S. Dysch[100], B.S. Dziedzic[85], Z.O. Earnshaw[145], B. Eckerova[28a], M.G. Eggleston[51], E. Egidio Purcino De Souza[81b], L.F. Ehrke[56], G. Eigen[16], K. Einsweiler[17a], T. Ekelof[159], P.A. Ekman[97], Y. El Ghazali[35b], H. El Jarrari[35e,147], A. El Moussaouy[35a], V. Ellajosyula[159], M. Ellert[159], F. Ellinghaus[169], A.A. Elliot[93], N. Ellis[36], J. Elmsheuser[29], M. Elsing[36], D. Emeliyanov[133], A. Emerman[41], Y. Enari[152], I. Ene[17a], S. Epari[13], J. Erdmann[49], A. Ereditato[19], P.A. Erland[85], M. Errenst[169], M. Escalier[66], C. Escobar[161], E. Etzion[150], G. Evans[129a], H. Evans[67], M.O. Evans[145], A. Ezhilov[37], S. Ezzarqtouni[35a], F. Fabbri[59], L. Fabbri[23b,23a], G. Facini[95], V. Fadeyev[135], R.M. Fakhrutdinov[37], S. Falciano[74a], P.J. Falke[24], S. Falke[36], J. Faltova[132], Y. Fan[14a], Y. Fang[14a,14d], G. Fanourakis[46], M. Fanti[70a,70b], M. Faraj[68a,68b], A. Farbin[8], A. Farilla[76a], T. Farooque[106], S.M. Farrington[52], F. Fassi[35e], D. Fassouliotis[9], M. Faucci Giannelli[75a,75b], W.J. Fawcett[32], L. Fayard[66], P. Federicova[130], O.L. Fedin[37,a], G. Fedotov[37], M. Feickert[160], L. Feligioni[101], A. Fell[138], D.E. Fellers[122], C. Feng[62b], M. Feng[14b], Z. Feng[113], M.J. Fenton[158], A.B. Fenyuk[37], L. Ferencz[48], S.W. Ferguson[45], J. Pretel[54], J. Ferrando[48], A. Ferrari[159], P. Ferrari[113], R. Ferrari[72a], D. Ferrere[56], C. Ferretti[105], F. Fiedler[99], A. Filipčič[92], E.K. Filmer[1], F. Filthaut[112], M.C.N. Fiolhais[129a,129c,b], L. Fiorini[161], F. Fischer[140], W.C. Fisher[106], T. Fitschen[20], I. Fleck[140], P. Fleischmann[105], T. Flick[169], L. Flores[127], M. Flores[33d], L.R. Flores Castillo[64a], F.M. Follega[77a,77b], N. Fomin[16], J.H. Foo[154], B.C. Forland[67], A. Formica[134], A.C. Forti[100], E. Fortin[101], A.W. Fortman[61], M.G. Foti[17a], L. Fountas[9], D. Fournier[66], H. Fox[90], P. Francavilla[73a,73b], S. Francescato[61], M. Franchini[23b,23a], S. Franchino[63a], D. Francis[36], L. Franco[112], L. Franconi[19], M. Franklin[61], G. Frattari[26], A.C. Freegard[93], P.M. Freeman[20], W.S. Freund[81b], N. Fritzsche[50], A. Froch[54], D. Froidevaux[36], J.A. Frost[125], Y. Fu[62a], M. Fujimoto[117], E. Fullana Torregrosa[161,*], J. Fuster[161], A. Gabrielli[23b,23a], A. Gabrielli[154], P. Gadow[48], G. Gagliardi[57b,57a], L.G. Gagnon[17a], G.E. Gallardo[125], E.J. Gallas[125], B.J. Gallop[133], R. Gamboa Goni[93], K.K. Gan[118], S. Ganguly[152], J. Gao[62a], Y. Gao[52], F.M. Garay Walls[136a,136b], B. Garcia[29,ad], C. García[161], J.E. García Navarro[161], J.A. García Pascual[14a], M. Garcia-Sciveres[17a], R.W. Gardner[39], D. Garg[79], R.B. Garg[142], S. Gargiulo[54], C.A. Garner[154],

V. Garonne[29], S.J. Gasiorowski[137], P. Gaspar[81b], G. Gaudio[72a], V. Gautam[13], P. Gauzzi[74a,74b], I.L. Gavrilenko[37], A. Gavrilyuk[37], C. Gay[162], G. Gaycken[48], E.N. Gazis[10], A.A. Geanta[27b,27e], C.M. Gee[135], J. Geisen[97], M. Geisen[99], C. Gemme[57b], M.H. Genest[60], S. Gentile[74a,74b], S. George[94], W.F. George[20], T. Geralis[46], L.O. Gerlach[55], P. Gessinger-Befurt[36], M. Ghasemi Bostanabad[163], M. Ghneimat[140], A. Ghosal[140], A. Ghosh[158], A. Ghosh[7], B. Giacobbe[23b], S. Giagu[74a,74b], N. Giangiacomi[154], P. Giannetti[73a], A. Giannini[62a], S.M. Gibson[94], M. Gignac[135], D.T. Gil[84b], A.K. Gilbert[84a], B.J. Gilbert[41], D. Gillberg[34], G. Gilles[113], N.E.K. Gillwald[48], L. Ginabat[126], D.M. Gingrich[2,aa], M.P. Giordani[68a,68c], P.F. Giraud[134], G. Giugliarelli[68a,68c], D. Giugni[70a], F. Giuli[36], I. Gkialas[9,i], L.K. Gladilin[37], C. Glasman[98], G.R. Gledhill[122], M. Glisic[122], I. Gnesi[43b,e], Y. Go[29,ad], M. Goblirsch-Kolb[26], D. Godin[107], S. Goldfarb[104], T. Golling[56], M.G.D. Gololo[33g], D. Golubkov[37], J.P. Gombas[106], A. Gomes[129a,129b], G. Gomes Da Silva[140], A.J. Gomez Delegido[161], R. Goncalves Gama[55], R. Gonçalo[129a,129c], G. Gonella[122], L. Gonella[20], A. Gongadze[38], F. Gonnella[20], J.L. Gonski[41], S. González de la Hoz[161], S. Gonzalez Fernandez[13], R. Gonzalez Lopez[91], C. Gonzalez Renteria[17a], R. Gonzalez Suarez[159], S. Gonzalez-Sevilla[56], G.R. Gonzalvo Rodriguez[161], R.Y. González Andana[52], L. Goossens[36], N.A. Gorasia[20], P.A. Gorbounov[37], B. Gorini[36], E. Gorini[69a,69b], A. Gorišek[92], A.T. Goshaw[51], M.I. Gostkin[38], C.A. Gottardo[36], M. Gouighri[35b], V. Goumarre[48], A.G. Goussiou[137], N. Govender[33c], C. Goy[4], I. Grabowska-Bold[84a], K. Graham[34], E. Gramstad[124], S. Grancagnolo[18], M. Grandi[145], V. Gratchev[37,*], P.M. Gravila[27f], F.G. Gravili[69a,69b], H.M. Gray[17a], M. Greco[69a,69b], C. Grefe[24], I.M. Gregor[48], P. Grenier[142], C. Grieco[13], A.A. Grillo[135], K. Grimm[31,m], S. Grinstein[13,t], J.-F. Grivaz[66], E. Gross[167], J. Grosse-Knetter[55], C. Grud[105], A. Grummer[111], J.C. Grundy[125], L. Guan[105], W. Guan[168], C. Gubbels[162], J.G.R. Guerrero Rojas[161], G. Guerrieri[68a,68b], F. Guescini[109], R. Gugel[99], J.A.M. Guhit[105], A. Guida[48], T. Guillemin[4], E. Guilloton[165,133], S. Guindon[36], F. Guo[14a,14d], J. Guo[62c], L. Guo[66], Y. Guo[105], R. Gupta[48], S. Gurbuz[24], S.S. Gurdasani[54], G. Gustavino[36], M. Guth[56], P. Gutierrez[119], L.F. Gutierrez Zagazeta[127], C. Gutschow[95], C. Guyot[134], C. Gwenlan[125], C.B. Gwilliam[91], E.S. Haaland[124], A. Haas[116], M. Habedank[48], C. Haber[17a], H.K. Hadavand[8], A. Hadef[99], S. Hadzic[109], M. Haleem[164], J. Haley[120], J.J. Hall[138], G.D. Hallewell[101], L. Halser[19], K. Hamano[163], H. Hamdaoui[35e], M. Hamer[24], G.N. Hamity[52], J. Han[62b], K. Han[62a], L. Han[14c], L. Han[62a], S. Han[17a], Y.F. Han[154], K. Hanagaki[82], M. Hance[135], D.A. Hangal[41,y], H. Hanif[141], M.D. Hank[39], R. Hankache[100], J.B. Hansen[42], J.D. Hansen[42], P.H. Hansen[42], K. Hara[156], D. Harada[56], T. Harenberg[169], S. Harkusha[37], Y.T. Harris[125], N.M. Harrison[118], P.F. Harrison[165], N.M. Hartman[142], N.M. Hartmann[108], Y. Hasegawa[139], A. Hasib[52], S. Haug[19], R. Hauser[106], M. Havranek[131], C.M. Hawkes[20], R.J. Hawkings[36], S. Hayashida[110], D. Hayden[106], C. Hayes[105], R.L. Hayes[162], C.P. Hays[125], J.M. Hays[93], H.S. Hayward[91], F. He[62a], Y. He[153], Y. He[126], M.P. Heath[52], V. Hedberg[97], A.L. Heggelund[124], N.D. Hehir[93], C. Heidegger[54], K.K. Heidegger[54], W.D. Heidorn[80], J. Heilman[34], S. Heim[48],

JHEP06(2023)191

T. Heim[17a], J.G. Heinlein[127], J.J. Heinrich[122], L. Heinrich[109], J. Hejbal[130], L. Helary[48], A. Held[168], S. Hellesund[124], C.M. Helling[162], S. Hellman[47a,47b], C. Helsens[36], R.C.W. Henderson[90], L. Henkelmann[32], A.M. Henriques Correia[36], H. Herde[142], Y. Hernández Jiménez[144], M.G. Herrmann[108], T. Herrmann[50], G. Herten[54], R. Hertenberger[108], L. Hervas[36], N.P. Hessey[155a], H. Hibi[83], E. Higón-Rodriguez[161], S.J. Hillier[20], I. Hinchliffe[17a], F. Hinterkeuser[24], M. Hirose[123], S. Hirose[156], D. Hirschbuehl[169], T.G. Hitchings[100], B. Hiti[92], J. Hobbs[144], R. Hobincu[27e], N. Hod[167], M.C. Hodgkinson[138], B.H. Hodkinson[32], A. Hoecker[36], J. Hofer[48], D. Hohn[54], T. Holm[24], M. Holzbock[109], L.B.A.H. Hommels[32], B.P. Honan[100], J. Hong[62c], T.M. Hong[128], Y. Hong[55], J.C. Honig[54], A. Hönle[109], B.H. Hooberman[160], W.H. Hopkins[6], Y. Horii[110], S. Hou[147], A.S. Howard[92], J. Howarth[59], J. Hoya[6], M. Hrabovsky[121], A. Hrynevich[37], T. Hryn'ova[4], P.J. Hsu[65], S.-C. Hsu[137], Q. Hu[41,y], Y.F. Hu[14a,14d,ac], D.P. Huang[95], S. Huang[64b], X. Huang[14c], Y. Huang[62a], Y. Huang[14a], Z. Huang[100], Z. Hubacek[131], M. Huebner[24], F. Huegging[24], T.B. Huffman[125], M. Huhtinen[36], S.K. Huiberts[16], R. Hulsken[103], N. Huseynov[12,a], J. Huston[106], J. Huth[61], R. Hyneman[142], S. Hyrych[28a], G. Iacobucci[56], G. Iakovidis[29], I. Ibragimov[140], L. Iconomidou-Fayard[66], P. Iengo[71a,71b], R. Iguchi[152], T. Iizawa[56], Y. Ikegami[82], A. Ilg[19], N. Ilic[154], H. Imam[35a], T. Ingebretsen Carlson[47a,47b], G. Introzzi[72a,72b], M. Iodice[76a], V. Ippolito[74a,74b], M. Ishino[152], W. Islam[168], C. Issever[18,48], S. Istin[21a,af], H. Ito[166], J.M. Iturbe Ponce[64a], R. Iuppa[77a,77b], A. Ivina[167], J.M. Izen[45], V. Izzo[71a], P. Jacka[130,131], P. Jackson[1], R.M. Jacobs[48], B.P. Jaeger[141], C.S. Jagfeld[108], G. Jäkel[169], K. Jakobs[54], T. Jakoubek[167], J. Jamieson[59], K.W. Janas[84a], G. Jarlskog[97], A.E. Jaspan[91], M. Javurkova[102], F. Jeanneau[134], L. Jeanty[122], J. Jejelava[148a,x], P. Jenni[54,f], C.E. Jessiman[34], S. Jézéquel[4], J. Jia[144], X. Jia[61], X. Jia[14a,14d], Z. Jia[14c], Y. Jiang[62a], S. Jiggins[52], J. Jimenez Pena[109], S. Jin[14c], A. Jinaru[27b], O. Jinnouchi[153], P. Johansson[138], K.A. Johns[7], D.M. Jones[32], E. Jones[165], P. Jones[32], R.W.L. Jones[90], T.J. Jones[91], R. Joshi[118], J. Jovicevic[15], X. Ju[17a], J.J. Junggeburth[36], A. Juste Rozas[13,t], S. Kabana[136e], A. Kaczmarska[85], M. Kado[74a,74b], H. Kagan[118], M. Kagan[142], A. Kahn[41], A. Kahn[127], C. Kahra[99], T. Kaji[166], E. Kajomovitz[149], N. Kakati[167], C.W. Kalderon[29], A. Kamenshchikov[154], S. Kanayama[153], N.J. Kang[135], Y. Kano[110], S. Kaphle[18], D. Kar[33g], K. Karava[125], M.J. Kareem[155b], E. Karentzos[54], I. Karkanias[151], S.N. Karpov[38], Z.M. Karpova[38], V. Kartvelishvili[90], A.N. Karyukhin[37], E. Kasimi[151], C. Kato[62d], J. Katzy[48], S. Kaur[34], K. Kawade[139], K. Kawagoe[88], T. Kawamoto[134], G. Kawamura[55], E.F. Kay[163], F.I. Kaya[157], S. Kazakos[13], V.F. Kazanin[37], Y. Ke[144], J.M. Keaveney[33a], R. Keeler[163], G.V. Kehris[61], J.S. Keller[34], A.S. Kelly[95], D. Kelsey[145], J.J. Kempster[20], K.E. Kennedy[41], O. Kepka[130], B.P. Kerridge[165], S. Kersten[169], B.P. Kerševan[92], S. Keshri[66], L. Keszeghova[28a], S. Ketabchi Haghighat[154], M. Khandoga[126], A. Khanov[120], A.G. Kharlamov[37], T. Kharlamova[37], E.E. Khoda[137], T.J. Khoo[18], G. Khoriauli[164], J. Khubua[148b], Y.A.R. Khwaira[66], M. Kiehn[36], A. Kilgallon[122], D.W. Kim[47a,47b], E. Kim[153], Y.K. Kim[39], N. Kimura[95], A. Kirchhoff[55], D. Kirchmeier[50], C. Kirfel[24], J. Kirk[133],

JHEP06(2023)191

A.E. Kiryunin[109], T. Kishimoto[152], D.P. Kisliuk[154], C. Kitsaki[10], O. Kivernyk[24], M. Klassen[63a], C. Klein[34], L. Klein[164], M.H. Klein[105], M. Klein[91], S.B. Klein[56], U. Klein[91], P. Klimek[36], A. Klimentov[29], F. Klimpel[109], T. Klingl[24], T. Klioutchnikova[36], F.F. Klitzner[108], P. Kluit[113], S. Kluth[109], E. Kneringer[78], T.M. Knight[154], A. Knue[54], D. Kobayashi[88], R. Kobayashi[86], M. Kocian[142], P. Kodyš[132], D.M. Koeck[145], P.T. Koenig[24], T. Koffas[34], N.M. Köhler[36], M. Kolb[134], I. Koletsou[4], T. Komarek[121], K. Köneke[54], A.X.Y. Kong[1], T. Kono[117], N. Konstantinidis[95], B. Konya[97], R. Kopeliansky[67], S. Koperny[84a], K. Korcyl[85], K. Kordas[151], G. Koren[150], A. Korn[95], S. Korn[55], I. Korolkov[13], N. Korotkova[37], B. Kortman[113], O. Kortner[109], S. Kortner[109], W.H. Kostecka[114], V.V. Kostyukhin[140], A. Kotsokechagia[134], A. Kotwal[51], A. Koulouris[36], A. Kourkoumeli-Charalampidi[72a,72b], C. Kourkoumelis[9], E. Kourlitis[6], O. Kovanda[145], R. Kowalewski[163], W. Kozanecki[134], A.S. Kozhin[37], V.A. Kramarenko[37], G. Kramberger[92], P. Kramer[99], M.W. Krasny[126], A. Krasznahorkay[36], J.A. Kremer[99], T. Kresse[50], J. Kretzschmar[91], K. Kreul[18], P. Krieger[154], F. Krieter[108], S. Krishnamurthy[102], A. Krishnan[63b], M. Krivos[132], K. Krizka[17a], K. Kroeninger[49], H. Kroha[109], J. Kroll[130], J. Kroll[127], K.S. Krowpman[106], U. Kruchonak[38], H. Krüger[24], N. Krumnack[80], M.C. Kruse[51], J.A. Krzysiak[85], A. Kubota[153], O. Kuchinskaia[37], S. Kuday[3a], D. Kuechler[48], J.T. Kuechler[48], S. Kuehn[36], T. Kuhl[48], V. Kukhtin[38], Y. Kulchitsky[37,a], S. Kuleshov[136d,136b], M. Kumar[33g], N. Kumari[101], M. Kuna[60], A. Kupco[130], T. Kupfer[49], A. Kupich[37], O. Kuprash[54], H. Kurashige[83], L.L. Kurchaninov[155a], Y.A. Kurochkin[37], A. Kurova[37], E.S. Kuwertz[36], M. Kuze[153], A.K. Kvam[102], J. Kvita[121], T. Kwan[103], K.W. Kwok[64a], N.G. Kyriacou[105], L.A.O. Laatu[101], C. Lacasta[161], F. Lacava[74a,74b], H. Lacker[18], D. Lacour[126], N.N. Lad[95], E. Ladygin[38], B. Laforge[126], T. Lagouri[136e], S. Lai[55], I.K. Lakomiec[84a], N. Lalloue[60], J.E. Lambert[119], S. Lammers[67], W. Lampl[7], C. Lampoudis[151], A.N. Lancaster[114], E. Lançon[29], U. Landgraf[54], M.P.J. Landon[93], V.S. Lang[54], R.J. Langenberg[102], A.J. Lankford[158], F. Lanni[36], K. Lantzsch[24], A. Lanza[72a], A. Lapertosa[57b,57a], J.F. Laporte[134], T. Lari[70a], F. Lasagni Manghi[23b], M. Lassnig[36], V. Latonova[130], T.S. Lau[64a], A. Laudrain[99], A. Laurier[34], S.D. Lawlor[94], Z. Lawrence[100], M. Lazzaroni[70a,70b], B. Le[100], B. Leban[92], A. Lebedev[80], M. LeBlanc[36], T. LeCompte[6], F. Ledroit-Guillon[60], A.C.A. Lee[95], G.R. Lee[16], L. Lee[61], S.C. Lee[147], S. Lee[47a,47b], T.F. Lee[91], L.L. Leeuw[33c], H.P. Lefebvre[94], M. Lefebvre[163], C. Leggett[17a], K. Lehmann[141], G. Lehmann Miotto[36], M. Leigh[56], W.A. Leight[102], A. Leisos[151,s], M.A.L. Leite[81c], C.E. Leitgeb[48], R. Leitner[132], K.J.C. Leney[44], T. Lenz[24], S. Leone[73a], C. Leonidopoulos[52], A. Leopold[143], C. Leroy[107], R. Les[106], C.G. Lester[32], M. Levchenko[37], J. Levêque[4], D. Levin[105], L.J. Levinson[167], M.P. Lewicki[85], D.J. Lewis[20], B. Li[14b], B. Li[62b], C. Li[62a], C-Q. Li[62c], H. Li[62a], H. Li[62b], H. Li[14c], H. Li[62b], J. Li[62c], K. Li[137], L. Li[62c], M. Li[14a,14d], Q.Y. Li[62a], S. Li[62d,62c,d], T. Li[62b], X. Li[103], Z. Li[62b], Z. Li[125], Z. Li[103], Z. Li[91], Z. Liang[14a], M. Liberatore[48], B. Liberti[75a], K. Lie[64c], J. Lieber Marin[81b], K. Lin[106], R.A. Linck[67], R.E. Lindley[7], J.H. Lindon[2], A. Linss[48], E. Lipeles[127], A. Lipniacka[16], A. Lister[162], J.D. Little[4], B. Liu[14a], B.X. Liu[141], D. Liu[62d,62c], J.B. Liu[62a],

JHEP06(2023)191

J.K.K. Liu [32], K. Liu [62d,62c], M. Liu [62a], M.Y. Liu [62a], P. Liu [14a], Q. Liu [62d,137,62c], X. Liu [62a], Y. Liu [48], Y. Liu [14c,14d], Y.L. Liu [105], Y.W. Liu [62a], M. Livan [72a,72b], J. Llorente Merino [141], S.L. Lloyd [93], E.M. Lobodzinska [48], P. Loch [7], S. Loffredo [75a,75b], T. Lohse [18], K. Lohwasser [138], M. Lokajicek [130], J.D. Long [160], I. Longarini [74a,74b], L. Longo [69a,69b], R. Longo [160], I. Lopez Paz [36], A. Lopez Solis [48], J. Lorenz [108], N. Lorenzo Martinez [4], A.M. Lory [108], A. Lösle [54], X. Lou [47a,47b], X. Lou [14a,14d], A. Lounis [66], J. Love [6], P.A. Love [90], J.J. Lozano Bahilo [161], G. Lu [14a,14d], M. Lu [79], S. Lu [127], Y.J. Lu [65], H.J. Lubatti [137], C. Luci [74a,74b], F.L. Lucio Alves [14c], A. Lucotte [60], F. Luehring [67], I. Luise [144], O. Lukianchuk [66], O. Lundberg [143], B. Lund-Jensen [143], N.A. Luongo [122], M.S. Lutz [150], D. Lynn [29], H. Lyons[91], R. Lysak [130], E. Lytken [97], F. Lyu [14a], V. Lyubushkin [38], T. Lyubushkina [38], H. Ma [29], L.L. Ma [62b], Y. Ma [95], D.M. Mac Donell [163], G. Maccarrone [53], J.C. MacDonald [138], R. Madar [40], W.F. Mader [50], J. Maeda [83], T. Maeno [29], M. Maerker [50], V. Magerl [54], J. Magro [68a,68c], H. Maguire [138], D.J. Mahon [41], C. Maidantchik [81b], A. Maio [129a,129b,129d], K. Maj [84a], O. Majersky [28a], S. Majewski [122], N. Makovec [66], V. Maksimovic [15], B. Malaescu [126], Pa. Malecki [85], V.P. Maleev [37], F. Malek [60], D. Malito [43b,43a], U. Mallik [79], C. Malone [32], S. Maltezos[10], S. Malyukov[38], J. Mamuzic [13], G. Mancini [53], G. Manco [72a,72b], J.P. Mandalia [93], I. Mandić [92], L. Manhaes de Andrade Filho [81a], I.M. Maniatis [151], M. Manisha [134], J. Manjarres Ramos [50], D.C. Mankad [167], A. Mann [108], B. Mansoulie [134], S. Manzoni [36], A. Marantis [151], G. Marchiori [5], M. Marcisovsky [130], L. Marcoccia [75a,75b], C. Marcon [70a,70b], M. Marinescu [20], M. Marjanovic [119], Z. Marshall [17a], S. Marti-Garcia [161], T.A. Martin [165], V.J. Martin [52], B. Martin dit Latour [16], L. Martinelli [74a,74b], M. Martinez [13,t], P. Martinez Agullo [161], V.I. Martinez Outschoorn [102], P. Martinez Suarez [13], S. Martin-Haugh [133], V.S. Martoiu [27b], A.C. Martyniuk [95], A. Marzin [36], S.R. Maschek [109], L. Masetti [99], T. Mashimo [152], J. Masik [100], A.L. Maslennikov [37], L. Massa [23b], P. Massarotti [71a,71b], P. Mastrandrea [73a,73b], A. Mastroberardino [43b,43a], T. Masubuchi [152], T. Mathisen [159], N. Matsuzawa[152], J. Maurer [27b], B. Maček [92], D.A. Maximov [37], R. Mazini [147], I. Maznas [151], M. Mazza [106], S.M. Mazza [135], C. Mc Ginn [29,ad], J.P. Mc Gowan [103], S.P. Mc Kee [105], T.G. McCarthy [109], W.P. McCormack [17a], E.F. McDonald [104], A.E. McDougall [113], J.A. Mcfayden [145], G. Mchedlidze [148b], R.P. Mckenzie [33g], T.C. Mclachlan [48], D.J. Mclaughlin [95], K.D. McLean [163], S.J. McMahon [133], P.C. McNamara [104], C.M. Mcpartland [91], R.A. McPherson [163,v], T. Megy [40], S. Mehlhase [108], A. Mehta [91], B. Meirose [45], D. Melini [149], B.R. Mellado Garcia [33g], A.H. Melo [55], F. Meloni [48], E.D. Mendes Gouveia [129a], A.M. Mendes Jacques Da Costa [20], H.Y. Meng [154], L. Meng [90], S. Menke [109], M. Mentink [36], E. Meoni [43b,43a], C. Merlassino [125], L. Merola [71a,71b], C. Meroni [70a], G. Merz[105], O. Meshkov [37], J.K.R. Meshreki [140], J. Metcalfe [6], A.S. Mete [6], C. Meyer [67], J-P. Meyer [134], M. Michetti [18], R.P. Middleton [133], L. Mijović [52], G. Mikenberg [167], M. Mikestikova [130], M. Mikuž [92], H. Mildner [138], A. Milic [154], C.D. Milke [44], D.W. Miller [39], L.S. Miller [34], A. Milov [167], D.A. Milstead[47a,47b], T. Min[14c], A.A. Minaenko [37], I.A. Minashvili [148b], L. Mince [59], A.I. Mincer [116], B. Mindur [84a], M. Mineev [38], Y. Mino [86], L.M. Mir [13], M. Miralles Lopez [161], M. Mironova [125], T. Mitani [166], A. Mitra [165], V.A. Mitsou [161],

O. Miu[154], P.S. Miyagawa[93], Y. Miyazaki[88], A. Mizukami[82], J.U. Mjörnmark[97], T. Mkrtchyan[63a], T. Mlinarevic[95], M. Mlynarikova[36], T. Moa[47a,47b], S. Mobius[55], K. Mochizuki[107], P. Moder[48], P. Mogg[108], A.F. Mohammed[14a,14d], S. Mohapatra[41], G. Mokgatitswane[33g], B. Mondal[140], S. Mondal[131], K. Mönig[48], E. Monnier[101], L. Monsonis Romero[161], J. Montejo Berlingen[36], M. Montella[118], F. Monticelli[89], N. Morange[66], A.L. Moreira De Carvalho[129a], M. Moreno Llácer[161], C. Moreno Martinez[13], P. Morettini[57b], S. Morgenstern[165], M. Morii[61], M. Morinaga[152], V. Morisbak[124], A.K. Morley[36], F. Morodei[74a,74b], L. Morvaj[36], P. Moschovakos[36], B. Moser[36], M. Mosidze[148b], T. Moskalets[54], P. Moskvitina[112], J. Moss[31,n], E.J.W. Moyse[102], S. Muanza[101], J. Mueller[128], D. Muenstermann[90], R. Müller[19], G.A. Mullier[97], J.J. Mullin[127], D.P. Mungo[70a,70b], J.L. Munoz Martinez[13], D. Munoz Perez[161], F.J. Munoz Sanchez[100], M. Murin[100], W.J. Murray[165,133], A. Murrone[70a,70b], J.M. Muse[119], M. Muškinja[17a], C. Mwewa[29], A.G. Myagkov[37,a], A.J. Myers[8], A.A. Myers[128], G. Myers[67], M. Myska[131], B.P. Nachman[17a], O. Nackenhorst[49], A. Nag[50], K. Nagai[125], K. Nagano[82], J.L. Nagle[29,ad], E. Nagy[101], A.M. Nairz[36], Y. Nakahama[82], K. Nakamura[82], H. Nanjo[123], R. Narayan[44], E.A. Narayanan[111], I. Naryshkin[37], M. Naseri[34], C. Nass[24], G. Navarro[22a], J. Navarro-Gonzalez[161], R. Nayak[150], A. Nayaz[18], P.Y. Nechaeva[37], F. Nechansky[48], L. Nedic[125], T.J. Neep[20], A. Negri[72a,72b], M. Negrini[23b], C. Nellist[112], C. Nelson[103], K. Nelson[105], S. Nemecek[130], M. Nessi[36,g], M.S. Neubauer[160], F. Neuhaus[99], J. Neundorf[48], R. Newhouse[162], P.R. Newman[20], C.W. Ng[128], Y.S. Ng[18], Y.W.Y. Ng[158], B. Ngair[35e], H.D.N. Nguyen[107], R.B. Nickerson[125], R. Nicolaidou[134], J. Nielsen[135], M. Niemeyer[55], N. Nikiforou[36], V. Nikolaenko[37,a], I. Nikolic-Audit[126], K. Nikolopoulos[20], P. Nilsson[29], H.R. Nindhito[56], A. Nisati[74a], N. Nishu[2], R. Nisius[109], J-E. Nitschke[50], E.K. Nkadimeng[33g], S.J. Noacco Rosende[89], T. Nobe[152], D.L. Noel[32], Y. Noguchi[86], T. Nommensen[146], M.A. Nomura[29], M.B. Norfolk[138], R.R.B. Norisam[95], B.J. Norman[34], J. Novak[92], T. Novak[48], O. Novgorodova[50], L. Novotny[131], R. Novotny[111], L. Nozka[121], K. Ntekas[158], E. Nurse[95], F.G. Oakham[34,aa], J. Ocariz[126], A. Ochi[83], I. Ochoa[129a], S. Oerdek[159], A. Ogrodnik[84a], A. Oh[100], C.C. Ohm[143], H. Oide[153], R. Oishi[152], M.L. Ojeda[48], Y. Okazaki[86], M.W. O'Keefe[91], Y. Okumura[152], A. Olariu[27b], L.F. Oleiro Seabra[129a], S.A. Olivares Pino[136e], D. Oliveira Damazio[29], D. Oliveira Goncalves[81a], J.L. Oliver[158], M.J.R. Olsson[158], A. Olszewski[85], J. Olszowska[85,*], Ö.O. Öncel[54], D.C. O'Neil[141], A.P. O'Neill[19], A. Onofre[129a,129e], P.U.E. Onyisi[11], M.J. Oreglia[39], G.E. Orellana[89], D. Orestano[76a,76b], N. Orlando[13], R.S. Orr[154], V. O'Shea[59], R. Ospanov[62a], G. Otero y Garzon[30], H. Otono[88], P.S. Ott[63a], G.J. Ottino[17a], M. Ouchrif[35d], J. Ouellette[29,ad], F. Ould-Saada[124], M. Owen[59], R.E. Owen[133], K.Y. Oyulmaz[21a], V.E. Ozcan[21a], N. Ozturk[8], S. Ozturk[21d], J. Pacalt[121], H.A. Pacey[32], K. Pachal[51], A. Pacheco Pages[13], C. Padilla Aranda[13], G. Padovano[74a,74b], S. Pagan Griso[17a], G. Palacino[67], A. Palazzo[69a,69b], S. Palazzo[52], S. Palestini[36], M. Palka[84b], J. Pan[170], T. Pan[64a], D.K. Panchal[11], C.E. Pandini[113], J.G. Panduro Vazquez[94], H. Pang[14b], P. Pani[48], G. Panizzo[68a,68c], L. Paolozzi[56], C. Papadatos[107], S. Parajuli[44], A. Paramonov[6], C. Paraskevopoulos[10], D. Paredes Hernandez[64b], T.H. Park[154],

JHEP06(2023)191

M.A. Parker[32], F. Parodi[57b,57a], E.W. Parrish[114], V.A. Parrish[52], J.A. Parsons[41], U. Parzefall[54], B. Pascual Dias[107], L. Pascual Dominguez[150], V.R. Pascuzzi[17a], F. Pasquali[113], E. Pasqualucci[74a], S. Passaggio[57b], F. Pastore[94], P. Pasuwan[47a,47b], P. Patel[85], J.R. Pater[100], J. Patton[91], T. Pauly[36], J. Pearkes[142], M. Pedersen[124], R. Pedro[129a], S.V. Peleganchuk[37], O. Penc[36], E.A. Pender[52], C. Peng[64b], H. Peng[62a], K.E. Penski[108], M. Penzin[37], B.S. Peralva[81d,81d], A.P. Pereira Peixoto[60], L. Pereira Sanchez[47a,47b], D.V. Perepelitsa[29,ad], E. Perez Codina[155a], M. Perganti[10], L. Perini[70a,70b,*], H. Pernegger[36], S. Perrella[36], A. Perrevoort[112], O. Perrin[40], K. Peters[48], R.F.Y. Peters[100], B.A. Petersen[36], T.C. Petersen[42], E. Petit[101], V. Petousis[131], C. Petridou[151], A. Petrukhin[140], M. Pettee[17a], N.E. Pettersson[36], A. Petukhov[37], K. Petukhova[132], A. Peyaud[134], R. Pezoa[136f], L. Pezzotti[36], G. Pezzullo[170], T.M. Pham[168], T. Pham[104], P.W. Phillips[133], M.W. Phipps[160], G. Piacquadio[144], E. Pianori[17a], F. Piazza[70a,70b], R. Piegaia[30], D. Pietreanu[27b], A.D. Pilkington[100], M. Pinamonti[68a,68c], J.L. Pinfold[2], B.C. Pinheiro Pereira[129a], C. Pitman Donaldson[95], D.A. Pizzi[34], L. Pizzimento[75a,75b], A. Pizzini[113], M.-A. Pleier[29], V. Plesanovs[54], V. Pleskot[132], E. Plotnikova[38], G. Poddar[4], R. Poettgen[97], L. Poggioli[126], I. Pogrebnyak[106], D. Pohl[24], I. Pokharel[55], S. Polacek[132], G. Polesello[72a], A. Poley[141,155a], R. Polifka[131], A. Polini[23b], C.S. Pollard[125], Z.B. Pollock[118], V. Polychronakos[29], E. Pompa Pacchi[74a,74b], D. Ponomarenko[37], L. Pontecorvo[36], S. Popa[27a], G.A. Popeneciu[27d], D.M. Portillo Quintero[155a], S. Pospisil[131], P. Postolache[27c], K. Potamianos[125], I.N. Potrap[38], C.J. Potter[32], H. Potti[1], T. Poulsen[48], J. Poveda[161], M.E. Pozo Astigarraga[36], A. Prades Ibanez[161], M.M. Prapa[46], D. Price[100], M. Primavera[69a], M.A. Principe Martin[98], M.L. Proffitt[137], N. Proklova[127], K. Prokofiev[64c], G. Proto[75a,75b], S. Protopopescu[29], J. Proudfoot[6], M. Przybycien[84a], J.E. Puddefoot[138], D. Pudzha[37], P. Puzo[66], D. Pyatiizbyantseva[37], J. Qian[105], Y. Qin[100], T. Qiu[93], A. Quadt[55], M. Queitsch-Maitland[100], G. Quetant[56], G. Rabanal Bolanos[61], D. Rafanoharana[54], F. Ragusa[70a,70b], J.L. Rainbolt[39], J.A. Raine[56], S. Rajagopalan[29], E. Ramakoti[37], K. Ran[48,14d], V. Raskina[126], D.F. Rassloff[63a], S. Rave[99], B. Ravina[55], I. Ravinovich[167], M. Raymond[36], A.L. Read[124], N.P. Readioff[138], D.M. Rebuzzi[72a,72b], G. Redlinger[29], K. Reeves[45], J.A. Reidelsturz[169], D. Reikher[150], A. Reiss[99], A. Rej[140], C. Rembser[36], A. Renardi[48], M. Renda[27b], M.B. Rendel[109], A.G. Rennie[59], S. Resconi[70a], M. Ressegotti[57b,57a], E.D. Resseguie[17a], S. Rettie[95], B. Reynolds[118], E. Reynolds[17a], M. Rezaei Estabragh[169], O.L. Rezanova[37], P. Reznicek[132], E. Ricci[77a,77b], R. Richter[109], S. Richter[47a,47b], E. Richter-Was[84b], M. Ridel[126], P. Rieck[116], P. Riedler[36], M. Rijssenbeek[144], A. Rimoldi[72a,72b], M. Rimoldi[48], L. Rinaldi[23b,23a], T.T. Rinn[29], M.P. Rinnagel[108], G. Ripellino[143], I. Riu[13], P. Rivadeneira[48], J.C. Rivera Vergara[163], F. Rizatdinova[120], E. Rizvi[93], C. Rizzi[56], B.A. Roberts[165], B.R. Roberts[17a], S.H. Robertson[103,v], M. Robin[48], D. Robinson[32], C.M. Robles Gajardo[136f], M. Robles Manzano[99], A. Robson[59], A. Rocchi[75a,75b], C. Roda[73a,73b], S. Rodriguez Bosca[63a], Y. Rodriguez Garcia[22a], A. Rodriguez Rodriguez[54], A.M. Rodríguez Vera[155b], S. Roe[36], J.T. Roemer[158], A.R. Roepe-Gier[119], J. Roggel[169], O. Røhne[124], R.A. Rojas[163], B. Roland[54], C.P.A. Roland[67], J. Roloff[29], A. Romaniouk[37], E. Romano[72a,72b],

M. Romano[23b], A.C. Romero Hernandez[160], N. Rompotis[91], L. Roos[126], S. Rosati[74a], B.J. Rosser[39], E. Rossi[4], E. Rossi[71a,71b], L.P. Rossi[57b], L. Rossini[48], R. Rosten[118], M. Rotaru[27b], B. Rottler[54], D. Rousseau[66], D. Rousso[32], G. Rovelli[72a,72b], A. Roy[160], A. Rozanov[101], Y. Rozen[149], X. Ruan[33g], A. Rubio Jimenez[161], A.J. Ruby[91], V.H. Ruelas Rivera[18], T.A. Ruggeri[1], F. Rühr[54], A. Ruiz-Martinez[161], A. Rummler[36], Z. Rurikova[54], N.A. Rusakovich[38], H.L. Russell[163], J.P. Rutherfoord[7], K. Rybacki[90], M. Rybar[132], E.B. Rye[124], A. Ryzhov[37], J.A. Sabater Iglesias[56], P. Sabatini[161], L. Sabetta[74a,74b], H.F-W. Sadrozinski[135], F. Safai Tehrani[74a], B. Safarzadeh Samani[145], M. Safdari[142], S. Saha[103], M. Sahinsoy[109], M. Saimpert[134], M. Saito[152], T. Saito[152], D. Salamani[36], G. Salamanna[76a,76b], A. Salnikov[142], J. Salt[161], A. Salvador Salas[13], D. Salvatore[43b,43a], F. Salvatore[145], A. Salzburger[36], D. Sammel[54], D. Sampsonidis[151], D. Sampsonidou[62d,62c], J. Sánchez[161], A. Sanchez Pineda[4], V. Sanchez Sebastian[161], H. Sandaker[124], C.O. Sander[48], J.A. Sandesara[102], M. Sandhoff[169], C. Sandoval[22b], D.P.C. Sankey[133], A. Sansoni[53], L. Santi[74a,74b], C. Santoni[40], H. Santos[129a,129b], S.N. Santpur[17a], A. Santra[167], K.A. Saoucha[138], J.G. Saraiva[129a,129d], J. Sardain[7], O. Sasaki[82], K. Sato[156], C. Sauer[63b], F. Sauerburger[54], E. Sauvan[4], P. Savard[154,aa], R. Sawada[152], C. Sawyer[133], L. Sawyer[96], I. Sayago Galvan[161], C. Sbarra[23b], A. Sbrizzi[23b,23a], T. Scanlon[95], J. Schaarschmidt[137], P. Schacht[109], D. Schaefer[39], U. Schäfer[99], A.C. Schaffer[66], D. Schaile[108], R.D. Schamberger[144], E. Schanet[108], C. Scharf[18], V.A. Schegelsky[37], D. Scheirich[132], F. Schenck[18], M. Schernau[158], C. Scheulen[55], C. Schiavi[57b,57a], Z.M. Schillaci[26], E.J. Schioppa[69a,69b], M. Schioppa[43b,43a], B. Schlag[99], K.E. Schleicher[54], S. Schlenker[36], K. Schmieden[99], C. Schmitt[99], S. Schmitt[48], L. Schoeffel[134], A. Schoening[63b], P.G. Scholer[54], E. Schopf[125], M. Schott[99], J. Schovancova[36], S. Schramm[56], F. Schroeder[169], H-C. Schultz-Coulon[63a], M. Schumacher[54], B.A. Schumm[135], Ph. Schune[134], A. Schwartzman[142], T.A. Schwarz[105], Ph. Schwemling[134], R. Schwienhorst[106], A. Sciandra[135], G. Sciolla[26], F. Scuri[73a], F. Scutti[104], C.D. Sebastiani[91], K. Sedlaczek[49], P. Seema[18], S.C. Seidel[111], A. Seiden[135], B.D. Seidlitz[41], T. Seiss[39], C. Seitz[48], J.M. Seixas[81b], G. Sekhniaidze[71a], S.J. Sekula[44], L. Selem[4], N. Semprini-Cesari[23b,23a], S. Sen[51], D. Sengupta[56], V. Senthilkumar[161], L. Serin[66], L. Serkin[68a,68b], M. Sessa[76a,76b], H. Severini[119], S. Sevova[142], F. Sforza[57b,57a], A. Sfyrla[56], E. Shabalina[55], R. Shaheen[143], J.D. Shahinian[127], N.W. Shaikh[47a,47b], D. Shaked Renous[167], L.Y. Shan[14a], M. Shapiro[17a], A. Sharma[36], A.S. Sharma[162], P. Sharma[79], S. Sharma[48], P.B. Shatalov[37], K. Shaw[145], S.M. Shaw[100], Q. Shen[62c,5], P. Sherwood[95], L. Shi[95], C.O. Shimmin[170], Y. Shimogama[166], J.D. Shinner[94], I.P.J. Shipsey[125], S. Shirabe[60], M. Shiyakova[38], J. Shlomi[167], M.J. Shochet[39], J. Shojaii[104], D.R. Shope[124], S. Shrestha[118,ae], E.M. Shrif[33g], M.J. Shroff[163], P. Sicho[130], A.M. Sickles[160], E. Sideras Haddad[33g], A. Sidoti[23b], F. Siegert[50], Dj. Sijacki[15], R. Sikora[84a], F. Sili[89], J.M. Silva[20], M.V. Silva Oliveira[36], S.B. Silverstein[47a], S. Simion[66], R. Simoniello[36], E.L. Simpson[59], N.D. Simpson[97], S. Simsek[21d], S. Sindhu[55], P. Sinervo[154], V. Sinetckii[37], S. Singh[141], S. Singh[154], S. Sinha[48], S. Sinha[33g], M. Sioli[23b,23a], I. Siral[122], S.Yu. Sivoklokov[37,*], J. Sjölin[47a,47b], A. Skaf[55], E. Skorda[97], P. Skubic[119], M. Slawinska[85], V. Smakhtin[167], B.H. Smart[133], J. Smiesko[36], S.Yu. Smirnov[37], Y. Smirnov[37], L.N. Smirnova[37,a], O. Smirnova[97], A.C. Smith[41], E.A. Smith[39], H.A. Smith[125], J.L. Smith[91], R. Smith[142], M. Smizanska[90], K. Smolek[131], A. Smykiewicz[85], A.A. Snesarev[37], H.L. Snoek[113], S. Snyder[29], R. Sobie[163,v], A. Soffer[150], C.A. Solans Sanchez[36], E.Yu. Soldatov[37], U. Soldevila[161], A.A. Solodkov[37], S. Solomon[54], A. Soloshenko[38], K. Solovieva[54], O.V. Solovyanov[37], V. Solovyev[37], P. Sommer[36], A. Sonay[13], W.Y. Song[155b], A. Sopczak[131], A.L. Sopio[95], F. Sopkova[28b], V. Sothilingam[63a], S. Sottocornola[72a,72b], R. Soualah[115c], Z. Soumaimi[35e], D. South[48], S. Spagnolo[69a,69b], M. Spalla[109], F. Spanò[94], D. Sperlich[54], G. Spigo[36], M. Spina[145], S. Spinali[90], D.P. Spiteri[59], M. Spousta[132], E.J. Staats[34], A. Stabile[70a,70b], R. Stamen[63a], M. Stamenkovic[113], A. Stampekis[20], M. Standke[24], E. Stanecka[85], M.V. Stange[50], B. Stanislaus[17a], M.M. Stanitzki[48], M. Stankaityte[125], B. Stapf[48], E.A. Starchenko[37], G.H. Stark[135], J. Stark[101], D.M. Starko[155b], P. Staroba[130], P. Starovoitov[63a], S. Stärz[103], R. Staszewski[85], G. Stavropoulos[46], J. Steentoft[159], P. Steinberg[29], A.L. Steinhebel[122], B. Stelzer[141,155a], H.J. Stelzer[128], O. Stelzer-Chilton[155a], H. Stenzel[58], T.J. Stevenson[145], G.A. Stewart[36], M.C. Stockton[36], G. Stoicea[27b], M. Stolarski[129a], S. Stonjek[109], A. Straessner[50], J. Strandberg[143], S. Strandberg[47a,47b], M. Strauss[119], T. Strebler[101], P. Strizenec[28b], R. Ströhmer[164], D.M. Strom[122], L.R. Strom[48], R. Stroynowski[44], A. Strubig[47a,47b], S.A. Stucci[29], B. Stugu[16], J. Stupak[119], N.A. Styles[48], D. Su[142], S. Su[62a], W. Su[62d,137,62c], X. Su[62a,66], K. Sugizaki[152], V.V. Sulin[37], M.J. Sullivan[91], D.M.S. Sultan[77a,77b], L. Sultanaliyeva[37], S. Sultansoy[3b], T. Sumida[86], S. Sun[105], S. Sun[168], O. Sunneborn Gudnadottir[159], M.R. Sutton[145], M. Svatos[130], M. Swiatlowski[155a], T. Swirski[164], I. Sykora[28a], M. Sykora[132], T. Sykora[132], D. Ta[99], K. Tackmann[48,u], A. Taffard[158], R. Tafirout[155a], J.S. Tafoya Vargas[66], R.H.M. Taibah[126], R. Takashima[87], K. Takeda[83], E.P. Takeva[52], Y. Takubo[82], M. Talby[101], A.A. Talyshev[37], K.C. Tam[64b], N.M. Tamir[150], A. Tanaka[152], J. Tanaka[152], R. Tanaka[66], M. Tanasini[57b,57a], J. Tang[62c], Z. Tao[162], S. Tapia Araya[80], S. Tapprogge[99], A. Tarek Abouelfadl Mohamed[106], S. Tarem[149], K. Tariq[62b], G. Tarna[27b], G.F. Tartarelli[70a], P. Tas[132], M. Tasevsky[130], E. Tassi[43b,43a], A.C. Tate[160], G. Tateno[152], Y. Tayalati[35e], G.N. Taylor[104], W. Taylor[155b], H. Teagle[91], A.S. Tee[168], R. Teixeira De Lima[142], P. Teixeira-Dias[94], J.J. Teoh[154], K. Terashi[152], J. Terron[98], S. Terzo[13], M. Testa[53], R.J. Teuscher[154,v], A. Thaler[78], O. Theiner[56], N. Themistokleous[52], T. Theveneaux-Pelzer[18], O. Thielmann[169], D.W. Thomas[94], J.P. Thomas[20], E.A. Thompson[48], P.D. Thompson[20], E. Thomson[127], E.J. Thorpe[93], Y. Tian[55], V. Tikhomirov[37,a], Yu.A. Tikhonov[37], S. Timoshenko[37], E.X.L. Ting[1], P. Tipton[170], S. Tisserant[101], S.H. Tlou[33g], A. Thourji[40], K. Todome[23b,23a], S. Todorova-Nova[132], S. Todt[50], M. Togawa[82], J. Tojo[88], S. Tokár[28a], K. Tokushuku[82], R. Tombs[32], M. Tomoto[82,110], L. Tompkins[142], K.W. Topolnicki[84b], P. Tornambe[102], E. Torrence[122], H. Torres[50], E. Torró Pastor[161], M. Toscani[30], C. Tosciri[39], D.R. Tovey[138], A. Traeet[16], I.S. Trandafir[27b], T. Trefzger[164], A. Tricoli[29], I.M. Trigger[155a], S. Trincaz-Duvoid[126], D.A. Trischuk[26], B. Trocmé[60], A. Trofymov[66], C. Troncon[70a], L. Truong[33c], M. Trzebinski[85], A. Trzupek[85], F. Tsai[144], M. Tsai[105], A. Tsiamis[151],

JHEP06(2023)191

P.V. Tsiareshka[37], S. Tsigaridas[155a], A. Tsirigotis[151,s], V. Tsiskaridze[144], E.G. Tskhadadze[148a], M. Tsopoulou[151], Y. Tsujikawa[86], I.I. Tsukerman[37], V. Tsulaia[17a], S. Tsuno[82], O. Tsur[149], D. Tsybychev[144], Y. Tu[64b], A. Tudorache[27b], V. Tudorache[27b], A.N. Tuna[36], S. Turchikhin[38], I. Turk Cakir[3a], R. Turra[70a], T. Turtuvshin[38], P.M. Tuts[41], S. Tzamarias[151], P. Tzanis[10], E. Tzovara[99], K. Uchida[152], F. Ukegawa[156], P.A. Ulloa Poblete[136c], G. Unal[36], M. Unal[11], A. Undrus[29], G. Unel[158], J. Urban[28b], P. Urquijo[104], G. Usai[8], R. Ushioda[153], M. Usman[107], Z. Uysal[21b], V. Vacek[131], B. Vachon[103], K.O.H. Vadla[124], T. Vafeiadis[36], C. Valderanis[108], E. Valdes Santurio[47a,47b], M. Valente[155a], S. Valentinetti[23b,23a], A. Valero[161], A. Vallier[101], J.A. Valls Ferrer[161], T.R. Van Daalen[137], P. Van Gemmeren[6], M. Van Rijnbach[124,36], S. Van Stroud[95], I. Van Vulpen[113], M. Vanadia[75a,75b], W. Vandelli[36], M. Vandenbroucke[134], E.R. Vandewall[120], D. Vannicola[150], L. Vannoli[57b,57a], R. Vari[74a], E.W. Varnes[7], C. Varni[17a], T. Varol[147], D. Varouchas[66], L. Varriale[161], K.E. Varvell[146], M.E. Vasile[27b], L. Vaslin[40], G.A. Vasquez[163], F. Vazeille[40], T. Vazquez Schroeder[36], J. Veatch[31], V. Vecchio[100], M.J. Veen[102], I. Veliscek[125], L.M. Veloce[154], F. Veloso[129a,129c], S. Veneziano[74a], A. Ventura[69a,69b], A. Verbytskyi[109], M. Verducci[73a,73b], C. Vergis[24], M. Verissimo De Araujo[81b], W. Verkerke[113], J.C. Vermeulen[113], C. Vernieri[142], P.J. Verschuuren[94], M. Vessella[102], M.C. Vetterli[141,aa], A. Vgenopoulos[151], N. Viaux Maira[136f], T. Vickey[138], O.E. Vickey Boeriu[138], G.H.A. Viehhauser[125], L. Vigani[63b], M. Villa[23b,23a], M. Villaplana Perez[161], E.M. Villhauer[52], E. Vilucchi[53], M.G. Vincter[34], G.S. Virdee[20], A. Vishwakarma[52], C. Vittori[23b,23a], I. Vivarelli[145], V. Vladimirov[165], E. Voevodina[109], F. Vogel[108], P. Vokac[131], J. Von Ahnen[48], E. Von Toerne[24], B. Vormwald[36], V. Vorobel[132], K. Vorobev[37], M. Vos[161], J.H. Vossebeld[91], M. Vozak[113], L. Vozdecky[93], N. Vranjes[15], M. Vranjes Milosavljevic[15], M. Vreeswijk[113], R. Vuillermet[36], O. Vujinovic[99], I. Vukotic[39], S. Wada[156], C. Wagner[102], W. Wagner[169], S. Wahdan[169], H. Wahlberg[89], R. Wakasa[156], M. Wakida[110], V.M. Walbrecht[109], J. Walder[133], R. Walker[108], W. Walkowiak[140], A.M. Wang[61], A.Z. Wang[168], C. Wang[62a], C. Wang[62c], H. Wang[17a], J. Wang[64a], P. Wang[44], R.-J. Wang[99], R. Wang[61], R. Wang[6], S.M. Wang[147], S. Wang[62b], T. Wang[62a], W.T. Wang[79], W.X. Wang[62a], X. Wang[14c], X. Wang[160], X. Wang[62c], Y. Wang[62d], Y. Wang[14c], Z. Wang[105], Z. Wang[62d,51,62c], Z. Wang[105], A. Warburton[103], R.J. Ward[20], N. Warrack[59], A.T. Watson[20], M.F. Watson[20], G. Watts[137], B.M. Waugh[95], A.F. Webb[11], C. Weber[29], M.S. Weber[19], S.M. Weber[63a], C. Wei[62a], Y. Wei[125], A.R. Weidberg[125], J. Weingarten[49], M. Weirich[99], C. Weiser[54], C.J. Wells[48], T. Wenaus[29], B. Wendland[49], T. Wengler[36], N.S. Wenke[109], N. Wermes[24], M. Wessels[63a], K. Whalen[122], A.M. Wharton[90], A.S. White[61], A. White[8], M.J. White[1], D. Whiteson[158], L. Wickremasinghe[123], W. Wiedenmann[168], C. Wiel[50], M. Wielers[133], N. Wieseotte[99], C. Wiglesworth[42], L.A.M. Wiik-Fuchs[54], D.J. Wilbern[119], H.G. Wilkens[36], D.M. Williams[41], H.H. Williams[127], S. Williams[32], S. Willocq[102], P.J. Windischhofer[125], F. Winklmeier[122], B.T. Winter[54], M. Wittgen[142], M. Wobisch[96], R. Wölker[125], J. Wollrath[158], M.W. Wolter[85], H. Wolters[129a,129c], V.W.S. Wong[162], A.F. Wongel[48], S.D. Worm[48], B.K. Wosiek[85], K.W. Woźniak[85],

JHEP06(2023)191

K. Wraight[59], J. Wu[14a,14d], M. Wu[64a], M. Wu[112], S.L. Wu[168], X. Wu[56], Y. Wu[62a], Z. Wu[134,62a], J. Wuerzinger[125], T.R. Wyatt[100], B.M. Wynne[52], S. Xella[42], L. Xia[14c], M. Xia[14b], J. Xiang[64c], X. Xiao[105], M. Xie[62a], X. Xie[62a], J. Xiong[17a], I. Xiotidis[145], D. Xu[14a], H. Xu[62a], H. Xu[62a], L. Xu[62a], R. Xu[127], T. Xu[105], W. Xu[105], Y. Xu[14b], Z. Xu[62b], Z. Xu[142], B. Yabsley[146], S. Yacoob[33a], N. Yamaguchi[88], Y. Yamaguchi[153], H. Yamauchi[156], T. Yamazaki[17a], Y. Yamazaki[83], J. Yan[62c], S. Yan[125], Z. Yan[25], H.J. Yang[62c,62d], H.T. Yang[17a], S. Yang[62a], T. Yang[64c], X. Yang[62a], X. Yang[14a], Y. Yang[44], Z. Yang[62a,105], W-M. Yao[17a], Y.C. Yap[48], H. Ye[14c], J. Ye[44], S. Ye[29], X. Ye[62a], Y. Yeh[95], I. Yeletskikh[38], M.R. Yexley[90], P. Yin[41], K. Yorita[166], C.J.S. Young[54], C. Young[142], M. Yuan[105], R. Yuan[62b,j], L. Yue[95], X. Yue[63a], M. Zaazoua[35e], B. Zabinski[85], E. Zaid[52], T. Zakareishvili[148b], N. Zakharchuk[34], S. Zambito[56], J.A. Zamora Saa[136d], J. Zang[152], D. Zanzi[54], O. Zaplatilek[131], S.V. Zeißner[49], C. Zeitnitz[169], J.C. Zeng[160], D.T. Zenger Jr[26], O. Zenin[37], T. Ženiš[28a], S. Zenz[93], S. Zerradi[35a], D. Zerwas[66], B. Zhang[14c], D.F. Zhang[138], G. Zhang[14b], J. Zhang[62b], J. Zhang[6], K. Zhang[14a,14d], L. Zhang[14c], P. Zhang[14a,14d], R. Zhang[168], S. Zhang[105], T. Zhang[152], X. Zhang[62c], X. Zhang[62b], Z. Zhang[17a], Z. Zhang[66], H. Zhao[137], P. Zhao[51], T. Zhao[62b], Y. Zhao[135], Z. Zhao[62a], A. Zhemchugov[38], X. Zheng[62a], Z. Zheng[142], D. Zhong[160], B. Zhou[105], C. Zhou[168], H. Zhou[7], N. Zhou[62c], Y. Zhou[7], C.G. Zhu[62b], C. Zhu[14a,14d], H.L. Zhu[62a], H. Zhu[14a], J. Zhu[105], Y. Zhu[62c], Y. Zhu[62a], X. Zhuang[14a], K. Zhukov[37], V. Zhulanov[37], N.I. Zimine[38], J. Zinsser[63b], M. Ziolkowski[140], L. Živković[15], A. Zoccoli[23b,23a], K. Zoch[56], T.G. Zorbas[138], O. Zormpa[46], W. Zou[41], L. Zwalinski[36]

[1] *Department of Physics, University of Adelaide, Adelaide; Australia*
[2] *Department of Physics, University of Alberta, Edmonton AB; Canada*
[3] [(a)] *Department of Physics, Ankara University, Ankara;* [(b)] *Division of Physics, TOBB University of Economics and Technology, Ankara; Türkiye*
[4] *LAPP, Univ. Savoie Mont Blanc, CNRS/IN2P3, Annecy; France*
[5] *APC, Université Paris Cité, CNRS/IN2P3, Paris; France*
[6] *High Energy Physics Division, Argonne National Laboratory, Argonne IL; United States of America*
[7] *Department of Physics, University of Arizona, Tucson AZ; United States of America*
[8] *Department of Physics, University of Texas at Arlington, Arlington TX; United States of America*
[9] *Physics Department, National and Kapodistrian University of Athens, Athens; Greece*
[10] *Physics Department, National Technical University of Athens, Zografou; Greece*
[11] *Department of Physics, University of Texas at Austin, Austin TX; United States of America*
[12] *Institute of Physics, Azerbaijan Academy of Sciences, Baku; Azerbaijan*
[13] *Institut de Física d'Altes Energies (IFAE), Barcelona Institute of Science and Technology, Barcelona; Spain*
[14] [(a)] *Institute of High Energy Physics, Chinese Academy of Sciences, Beijing;* [(b)] *Physics Department, Tsinghua University, Beijing;* [(c)] *Department of Physics, Nanjing University, Nanjing;* [(d)] *University of Chinese Academy of Science (UCAS), Beijing; China*
[15] *Institute of Physics, University of Belgrade, Belgrade; Serbia*
[16] *Department for Physics and Technology, University of Bergen, Bergen; Norway*
[17] [(a)] *Physics Division, Lawrence Berkeley National Laboratory, Berkeley CA;* [(b)] *University of California, Berkeley CA; United States of America*
[18] *Institut für Physik, Humboldt Universität zu Berlin, Berlin; Germany*
[19] *Albert Einstein Center for Fundamental Physics and Laboratory for High Energy Physics, University of Bern, Bern; Switzerland*

JHEP06(2023)191

[20] School of Physics and Astronomy, University of Birmingham, Birmingham; United Kingdom
[21] [(a)] Department of Physics, Bogazici University, Istanbul; [(b)] Department of Physics Engineering, Gaziantep University, Gaziantep; [(c)] Department of Physics, Istanbul University, Istanbul; [(d)] Istinye University, Sariyer, Istanbul; Türkiye
[22] [(a)] Facultad de Ciencias y Centro de Investigaciónes, Universidad Antonio Nariño, Bogotá; [(b)] Departamento de Física, Universidad Nacional de Colombia, Bogotá; Colombia
[23] [(a)] Dipartimento di Fisica e Astronomia A. Righi, Università di Bologna, Bologna; [(b)] INFN Sezione di Bologna; Italy
[24] Physikalisches Institut, Universität Bonn, Bonn; Germany
[25] Department of Physics, Boston University, Boston MA; United States of America
[26] Department of Physics, Brandeis University, Waltham MA; United States of America
[27] [(a)] Transilvania University of Brasov, Brasov; [(b)] Horia Hulubei National Institute of Physics and Nuclear Engineering, Bucharest; [(c)] Department of Physics, Alexandru Ioan Cuza University of Iasi, Iasi; [(d)] National Institute for Research and Development of Isotopic and Molecular Technologies, Physics Department, Cluj-Napoca; [(e)] University Politehnica Bucharest, Bucharest; [(f)] West University in Timisoara, Timisoara; [(g)] Faculty of Physics, University of Bucharest, Bucharest; Romania
[28] [(a)] Faculty of Mathematics, Physics and Informatics, Comenius University, Bratislava; [(b)] Department of Subnuclear Physics, Institute of Experimental Physics of the Slovak Academy of Sciences, Kosice; Slovak Republic
[29] Physics Department, Brookhaven National Laboratory, Upton NY; United States of America
[30] Universidad de Buenos Aires, Facultad de Ciencias Exactas y Naturales, Departamento de Física, y CONICET, Instituto de Física de Buenos Aires (IFIBA), Buenos Aires; Argentina
[31] California State University, CA; United States of America
[32] Cavendish Laboratory, University of Cambridge, Cambridge; United Kingdom
[33] [(a)] Department of Physics, University of Cape Town, Cape Town; [(b)] iThemba Labs, Western Cape; [(c)] Department of Mechanical Engineering Science, University of Johannesburg, Johannesburg; [(d)] National Institute of Physics, University of the Philippines Diliman (Philippines); [(e)] University of South Africa, Department of Physics, Pretoria; [(f)] University of Zululand, KwaDlangezwa; [(g)] School of Physics, University of the Witwatersrand, Johannesburg; South Africa
[34] Department of Physics, Carleton University, Ottawa ON; Canada
[35] [(a)] Faculté des Sciences Ain Chock, Réseau Universitaire de Physique des Hautes Energies — Université Hassan II, Casablanca; [(b)] Faculté des Sciences, Université Ibn-Tofail, Kénitra; [(c)] Faculté des Sciences Semlalia, Université Cadi Ayyad, LPHEA-Marrakech; [(d)] LPMR, Faculté des Sciences, Université Mohamed Premier, Oujda; [(e)] Faculté des sciences, Université Mohammed V, Rabat; [(f)] Institute of Applied Physics, Mohammed VI Polytechnic University, Ben Guerir; Morocco
[36] CERN, Geneva; Switzerland
[37] Affiliated with an institute covered by a cooperation agreement with CERN
[38] Affiliated with an international laboratory covered by a cooperation agreement with CERN
[39] Enrico Fermi Institute, University of Chicago, Chicago IL; United States of America
[40] LPC, Université Clermont Auvergne, CNRS/IN2P3, Clermont-Ferrand; France
[41] Nevis Laboratory, Columbia University, Irvington NY; United States of America
[42] Niels Bohr Institute, University of Copenhagen, Copenhagen; Denmark
[43] [(a)] Dipartimento di Fisica, Università della Calabria, Rende; [(b)] INFN Gruppo Collegato di Cosenza, Laboratori Nazionali di Frascati; Italy
[44] Physics Department, Southern Methodist University, Dallas TX; United States of America
[45] Physics Department, University of Texas at Dallas, Richardson TX; United States of America
[46] National Centre for Scientific Research "Demokritos", Agia Paraskevi; Greece
[47] [(a)] Department of Physics, Stockholm University; [(b)] Oskar Klein Centre, Stockholm; Sweden
[48] Deutsches Elektronen-Synchrotron DESY, Hamburg and Zeuthen; Germany
[49] Fakultät Physik, Technische Universität Dortmund, Dortmund; Germany
[50] Institut für Kern- und Teilchenphysik, Technische Universität Dresden, Dresden; Germany
[51] Department of Physics, Duke University, Durham NC; United States of America

JHEP06(2023)191

[52] *SUPA — School of Physics and Astronomy, University of Edinburgh, Edinburgh; United Kingdom*
[53] *INFN e Laboratori Nazionali di Frascati, Frascati; Italy*
[54] *Physikalisches Institut, Albert-Ludwigs-Universität Freiburg, Freiburg; Germany*
[55] *II. Physikalisches Institut, Georg-August-Universität Göttingen, Göttingen; Germany*
[56] *Département de Physique Nucléaire et Corpusculaire, Université de Genève, Genève; Switzerland*
[57] *[(a)] Dipartimento di Fisica, Università di Genova, Genova; [(b)] INFN Sezione di Genova; Italy*
[58] *II. Physikalisches Institut, Justus-Liebig-Universität Giessen, Giessen; Germany*
[59] *SUPA — School of Physics and Astronomy, University of Glasgow, Glasgow; United Kingdom*
[60] *LPSC, Université Grenoble Alpes, CNRS/IN2P3, Grenoble INP, Grenoble; France*
[61] *Laboratory for Particle Physics and Cosmology, Harvard University, Cambridge MA; United States of America*
[62] *[(a)] Department of Modern Physics and State Key Laboratory of Particle Detection and Electronics, University of Science and Technology of China, Hefei; [(b)] Institute of Frontier and Interdisciplinary Science and Key Laboratory of Particle Physics and Particle Irradiation (MOE), Shandong University, Qingdao; [(c)] School of Physics and Astronomy, Shanghai Jiao Tong University, Key Laboratory for Particle Astrophysics and Cosmology (MOE), SKLPPC, Shanghai; [(d)] Tsung-Dao Lee Institute, Shanghai; China*
[63] *[(a)] Kirchhoff-Institut für Physik, Ruprecht-Karls-Universität Heidelberg, Heidelberg; [(b)] Physikalisches Institut, Ruprecht-Karls-Universität Heidelberg, Heidelberg; Germany*
[64] *[(a)] Department of Physics, Chinese University of Hong Kong, Shatin, N.T., Hong Kong; [(b)] Department of Physics, University of Hong Kong, Hong Kong; [(c)] Department of Physics and Institute for Advanced Study, Hong Kong University of Science and Technology, Clear Water Bay, Kowloon, Hong Kong; China*
[65] *Department of Physics, National Tsing Hua University, Hsinchu; Taiwan*
[66] *IJCLab, Université Paris-Saclay, CNRS/IN2P3, 91405, Orsay; France*
[67] *Department of Physics, Indiana University, Bloomington IN; United States of America*
[68] *[(a)] INFN Gruppo Collegato di Udine, Sezione di Trieste, Udine; [(b)] ICTP, Trieste; [(c)] Dipartimento Politecnico di Ingegneria e Architettura, Università di Udine, Udine; Italy*
[69] *[(a)] INFN Sezione di Lecce; [(b)] Dipartimento di Matematica e Fisica, Università del Salento, Lecce; Italy*
[70] *[(a)] INFN Sezione di Milano; [(b)] Dipartimento di Fisica, Università di Milano, Milano; Italy*
[71] *[(a)] INFN Sezione di Napoli; [(b)] Dipartimento di Fisica, Università di Napoli, Napoli; Italy*
[72] *[(a)] INFN Sezione di Pavia; [(b)] Dipartimento di Fisica, Università di Pavia, Pavia; Italy*
[73] *[(a)] INFN Sezione di Pisa; [(b)] Dipartimento di Fisica E. Fermi, Università di Pisa, Pisa; Italy*
[74] *[(a)] INFN Sezione di Roma; [(b)] Dipartimento di Fisica, Sapienza Università di Roma, Roma; Italy*
[75] *[(a)] INFN Sezione di Roma Tor Vergata; [(b)] Dipartimento di Fisica, Università di Roma Tor Vergata, Roma; Italy*
[76] *[(a)] INFN Sezione di Roma Tre; [(b)] Dipartimento di Matematica e Fisica, Università Roma Tre, Roma; Italy*
[77] *[(a)] INFN-TIFPA; [(b)] Università degli Studi di Trento, Trento; Italy*
[78] *Universität Innsbruck, Department of Astro and Particle Physics, Innsbruck; Austria*
[79] *University of Iowa, Iowa City IA; United States of America*
[80] *Department of Physics and Astronomy, Iowa State University, Ames IA; United States of America*
[81] *[(a)] Departamento de Engenharia Elétrica, Universidade Federal de Juiz de Fora (UFJF), Juiz de Fora; [(b)] Universidade Federal do Rio De Janeiro COPPE/EE/IF, Rio de Janeiro; [(c)] Instituto de Física, Universidade de São Paulo, São Paulo; [(d)] Rio de Janeiro State University, Rio de Janeiro; Brazil*
[82] *KEK, High Energy Accelerator Research Organization, Tsukuba; Japan*
[83] *Graduate School of Science, Kobe University, Kobe; Japan*
[84] *[(a)] AGH University of Science and Technology, Faculty of Physics and Applied Computer Science, Krakow; [(b)] Marian Smoluchowski Institute of Physics, Jagiellonian University, Krakow; Poland*
[85] *Institute of Nuclear Physics Polish Academy of Sciences, Krakow; Poland*
[86] *Faculty of Science, Kyoto University, Kyoto; Japan*
[87] *Kyoto University of Education, Kyoto; Japan*

[88] *Research Center for Advanced Particle Physics and Department of Physics, Kyushu University, Fukuoka; Japan*
[89] *Instituto de Física La Plata, Universidad Nacional de La Plata and CONICET, La Plata; Argentina*
[90] *Physics Department, Lancaster University, Lancaster; United Kingdom*
[91] *Oliver Lodge Laboratory, University of Liverpool, Liverpool; United Kingdom*
[92] *Department of Experimental Particle Physics, Jožef Stefan Institute and Department of Physics, University of Ljubljana, Ljubljana; Slovenia*
[93] *School of Physics and Astronomy, Queen Mary University of London, London; United Kingdom*
[94] *Department of Physics, Royal Holloway University of London, Egham; United Kingdom*
[95] *Department of Physics and Astronomy, University College London, London; United Kingdom*
[96] *Louisiana Tech University, Ruston LA; United States of America*
[97] *Fysiska institutionen, Lunds universitet, Lund; Sweden*
[98] *Departamento de Física Teorica C-15 and CIAFF, Universidad Autónoma de Madrid, Madrid; Spain*
[99] *Institut für Physik, Universität Mainz, Mainz; Germany*
[100] *School of Physics and Astronomy, University of Manchester, Manchester; United Kingdom*
[101] *CPPM, Aix-Marseille Université, CNRS/IN2P3, Marseille; France*
[102] *Department of Physics, University of Massachusetts, Amherst MA; United States of America*
[103] *Department of Physics, McGill University, Montreal QC; Canada*
[104] *School of Physics, University of Melbourne, Victoria; Australia*
[105] *Department of Physics, University of Michigan, Ann Arbor MI; United States of America*
[106] *Department of Physics and Astronomy, Michigan State University, East Lansing MI; United States of America*
[107] *Group of Particle Physics, University of Montreal, Montreal QC; Canada*
[108] *Fakultät für Physik, Ludwig-Maximilians-Universität München, München; Germany*
[109] *Max-Planck-Institut für Physik (Werner-Heisenberg-Institut), München; Germany*
[110] *Graduate School of Science and Kobayashi-Maskawa Institute, Nagoya University, Nagoya; Japan*
[111] *Department of Physics and Astronomy, University of New Mexico, Albuquerque NM; United States of America*
[112] *Institute for Mathematics, Astrophysics and Particle Physics, Radboud University/Nikhef, Nijmegen; Netherlands*
[113] *Nikhef National Institute for Subatomic Physics and University of Amsterdam, Amsterdam; Netherlands*
[114] *Department of Physics, Northern Illinois University, DeKalb IL; United States of America*
[115] [(a)] *New York University Abu Dhabi, Abu Dhabi;* [(b)] *United Arab Emirates University, Al Ain;* [(c)] *University of Sharjah, Sharjah; United Arab Emirates*
[116] *Department of Physics, New York University, New York NY; United States of America*
[117] *Ochanomizu University, Otsuka, Bunkyo-ku, Tokyo; Japan*
[118] *Ohio State University, Columbus OH; United States of America*
[119] *Homer L. Dodge Department of Physics and Astronomy, University of Oklahoma, Norman OK; United States of America*
[120] *Department of Physics, Oklahoma State University, Stillwater OK; United States of America*
[121] *Palacký University, Joint Laboratory of Optics, Olomouc; Czech Republic*
[122] *Institute for Fundamental Science, University of Oregon, Eugene, OR; United States of America*
[123] *Graduate School of Science, Osaka University, Osaka; Japan*
[124] *Department of Physics, University of Oslo, Oslo; Norway*
[125] *Department of Physics, Oxford University, Oxford; United Kingdom*
[126] *LPNHE, Sorbonne Université, Université Paris Cité, CNRS/IN2P3, Paris; France*
[127] *Department of Physics, University of Pennsylvania, Philadelphia PA; United States of America*
[128] *Department of Physics and Astronomy, University of Pittsburgh, Pittsburgh PA; United States of America*
[129] [(a)] *Laboratório de Instrumentação e Física Experimental de Partículas — LIP, Lisboa;* [(b)] *Departamento de Física, Faculdade de Ciências, Universidade de Lisboa, Lisboa;* [(c)] *Departamento*

JHEP06(2023)191

de Física, Universidade de Coimbra, Coimbra; [(d)] Centro de Física Nuclear da Universidade de Lisboa, Lisboa; [(e)] Departamento de Física, Universidade do Minho, Braga; [(f)] Departamento de Física Teórica y del Cosmos, Universidad de Granada, Granada (Spain); [(g)] Departamento de Física, Instituto Superior Técnico, Universidade de Lisboa, Lisboa; Portugal

[130] Institute of Physics of the Czech Academy of Sciences, Prague; Czech Republic

[131] Czech Technical University in Prague, Prague; Czech Republic

[132] Charles University, Faculty of Mathematics and Physics, Prague; Czech Republic

[133] Particle Physics Department, Rutherford Appleton Laboratory, Didcot; United Kingdom

[134] IRFU, CEA, Université Paris-Saclay, Gif-sur-Yvette; France

[135] Santa Cruz Institute for Particle Physics, University of California Santa Cruz, Santa Cruz CA; United States of America

[136] [(a)] Departamento de Física, Pontificia Universidad Católica de Chile, Santiago; [(b)] Millennium Institute for Subatomic physics at high energy frontier (SAPHIR), Santiago; [(c)] Instituto de Investigación Multidisciplinario en Ciencia y Tecnología, y Departamento de Física, Universidad de La Serena; [(d)] Universidad Andres Bello, Department of Physics, Santiago; [(e)] Instituto de Alta Investigación, Universidad de Tarapacá, Arica; [(f)] Departamento de Física, Universidad Técnica Federico Santa María, Valparaíso; Chile

[137] Department of Physics, University of Washington, Seattle WA; United States of America

[138] Department of Physics and Astronomy, University of Sheffield, Sheffield; United Kingdom

[139] Department of Physics, Shinshu University, Nagano; Japan

[140] Department Physik, Universität Siegen, Siegen; Germany

[141] Department of Physics, Simon Fraser University, Burnaby BC; Canada

[142] SLAC National Accelerator Laboratory, Stanford CA; United States of America

[143] Department of Physics, Royal Institute of Technology, Stockholm; Sweden

[144] Departments of Physics and Astronomy, Stony Brook University, Stony Brook NY; United States of America

[145] Department of Physics and Astronomy, University of Sussex, Brighton; United Kingdom

[146] School of Physics, University of Sydney, Sydney; Australia

[147] Institute of Physics, Academia Sinica, Taipei; Taiwan

[148] [(a)] E. Andronikashvili Institute of Physics, Iv. Javakhishvili Tbilisi State University, Tbilisi; [(b)] High Energy Physics Institute, Tbilisi State University, Tbilisi; [(c)] University of Georgia, Tbilisi; Georgia

[149] Department of Physics, Technion, Israel Institute of Technology, Haifa; Israel

[150] Raymond and Beverly Sackler School of Physics and Astronomy, Tel Aviv University, Tel Aviv; Israel

[151] Department of Physics, Aristotle University of Thessaloniki, Thessaloniki; Greece

[152] International Center for Elementary Particle Physics and Department of Physics, University of Tokyo, Tokyo; Japan

[153] Department of Physics, Tokyo Institute of Technology, Tokyo; Japan

[154] Department of Physics, University of Toronto, Toronto ON; Canada

[155] [(a)] TRIUMF, Vancouver BC; [(b)] Department of Physics and Astronomy, York University, Toronto ON; Canada

[156] Division of Physics and Tomonaga Center for the History of the Universe, Faculty of Pure and Applied Sciences, University of Tsukuba, Tsukuba; Japan

[157] Department of Physics and Astronomy, Tufts University, Medford MA; United States of America

[158] Department of Physics and Astronomy, University of California Irvine, Irvine CA; United States of America

[159] Department of Physics and Astronomy, University of Uppsala, Uppsala; Sweden

[160] Department of Physics, University of Illinois, Urbana IL; United States of America

[161] Instituto de Física Corpuscular (IFIC), Centro Mixto Universidad de Valencia — CSIC, Valencia; Spain

[162] Department of Physics, University of British Columbia, Vancouver BC; Canada

[163] Department of Physics and Astronomy, University of Victoria, Victoria BC; Canada

[164] Fakultät für Physik und Astronomie, Julius-Maximilians-Universität Würzburg, Würzburg; Germany

[165] Department of Physics, University of Warwick, Coventry; United Kingdom
[166] Waseda University, Tokyo; Japan
[167] Department of Particle Physics and Astrophysics, Weizmann Institute of Science, Rehovot; Israel
[168] Department of Physics, University of Wisconsin, Madison WI; United States of America
[169] Fakultät für Mathematik und Naturwissenschaften, Fachgruppe Physik, Bergische Universität Wuppertal, Wuppertal; Germany
[170] Department of Physics, Yale University, New Haven CT; United States of America

[a] Also Affiliated with an institute covered by a cooperation agreement with CERN
[b] Also at Borough of Manhattan Community College, City University of New York, New York NY; United States of America
[c] Also at Bruno Kessler Foundation, Trento; Italy
[d] Also at Center for High Energy Physics, Peking University; China
[e] Also at Centro Studi e Ricerche Enrico Fermi; Italy
[f] Also at CERN, Geneva; Switzerland
[g] Also at Département de Physique Nucléaire et Corpusculaire, Université de Genève, Genève; Switzerland
[h] Also at Departament de Fisica de la Universitat Autonoma de Barcelona, Barcelona; Spain
[i] Also at Department of Financial and Management Engineering, University of the Aegean, Chios; Greece
[j] Also at Department of Physics and Astronomy, Michigan State University, East Lansing MI; United States of America
[k] Also at Department of Physics and Astronomy, University of Louisville, Louisville, KY; United States of America
[l] Also at Department of Physics, Ben Gurion University of the Negev, Beer Sheva; Israel
[m] Also at Department of Physics, California State University, East Bay; United States of America
[n] Also at Department of Physics, California State University, Sacramento; United States of America
[o] Also at Department of Physics, King's College London, London; United Kingdom
[p] Also at Department of Physics, University of Fribourg, Fribourg; Switzerland
[q] Also at Department of Physics, University of Thessaly; Greece
[r] Also at Department of Physics, Westmont College, Santa Barbara; United States of America
[s] Also at Hellenic Open University, Patras; Greece
[t] Also at Institucio Catalana de Recerca i Estudis Avancats, ICREA, Barcelona; Spain
[u] Also at Institut für Experimentalphysik, Universität Hamburg, Hamburg; Germany
[v] Also at Institute of Particle Physics (IPP); Canada
[w] Also at Institute of Physics, Azerbaijan Academy of Sciences, Baku; Azerbaijan
[x] Also at Institute of Theoretical Physics, Ilia State University, Tbilisi; Georgia
[y] Also at Lawrence Livermore National Laboratory, Livermore; United States of America
[z] Also at The Collaborative Innovation Center of Quantum Matter (CICQM), Beijing; China
[aa] Also at TRIUMF, Vancouver BC; Canada
[ab] Also at Università di Napoli Parthenope, Napoli; Italy
[ac] Also at University of Chinese Academy of Sciences (UCAS), Beijing; China
[ad] Also at University of Colorado Boulder, Department of Physics, Colorado; United States of America
[ae] Also at Washington College, Maryland; United States of America
[af] Also at Yeditepe University, Physics Department, Istanbul; Türkiye
[ag] Also at Physics Department, An-Najah National University, Nablus; Palestine
[*] Deceased

JHEP06(2023)191